REDUCTION OF LARGE KINETIC MECHANISM OF N-HEPTANE USING DIRECTED RELATION GRAPH AND COMPUTATIONAL SINGULAR PERTURBATION METHODS

by

Oğuz Ulutürk

B.S., Mechanical Engineering, Yıldız Technical University, 2011

Submitted to the Institute for Graduate Studies in
Science and Engineering in partial fulfillment of
the requirements for the degree of
Master of Science

Graduate Program in Mechanical Engineering

Boğaziçi University

2015

ACKNOWLEDGEMENTS

I would like to state my gratitude to my thesis supervisor Assoc. Prof. Hasan Bedir. I am very thankful him for his guidance and encouragement during my thesis period. Also; I would like to thank my committee members Assoc. Prof. Kunt Atalık and Prof. Dr. Ramazan Yıldırım. I,also, want to thank my mother Şazimet Ulutürk, my father Ali Ulutürk, my sister Merve Ulutürk and my grandmother Emine Sengülenç for their greatest support, encouragement and love that felt me the luckiest person alive. I wish thank to my beloved friends Alpay Asma,Oğuzhan Aydınlı, Göker Külüşlü, Yasin Yeşilyurt and Cebrail Yıldırım for their friendship and encouragement not only in academic life but also in my special life for being there whenever I needed. I,also, want to express my sincere gratitude to TÜBİTAK that allows me to pursue my academic career in Bogazici university with their scholarship. Finally, I would like to express my sincere gratitude to Serap Çakıcı Alparslan for her support and guidance which taught me a lot of thing.

ABSTRACT

REDUCTION OF LARGE KINETIC MECHANISM OF N-HEPTANE USING DIRECTED RELATION GRAPH AND COMPUTATIONAL SINGULAR PERTURBATION METHODS

Increasing demand on energy makes scientists and engineers enthusiastic to find new and efficient ways while designing new engines. For this purpose, a tremendous effort is paid on fossil fuels which have an important role in energy field. Simulating fuels in computers is one of the most significant and useful methods in design and calculations thanks to it's cheapness and time efficiency. One of the most important points in here is that the reliability of the data used in the simulations. In this context, simulating fuels by using detailed mechanism taking both the all species and reactions occured during combustion into account is needed. However, working with the detailed system is only waste of time related to their level of detail. In this thesis, reduction of detailed mechanism of one of the most acknowledged diesel surrogate fuel called as n-heptane including 654 species and 4846 reversible reactions, is made. In this context, firstly the Directed Relation Graph Method has been applied for the adiabatic ignition results of n-heptane for wide range of conditions in terms of temperature, pressure, and stochiometry. In the end, skeletal mechanism that include 135 species and 1309 reactions is obtained. In addition, with the aim of eliminating the stifness, time scale analysis is utilized via using computational singular perturbation method. By this way, it is possible to eliminate stifness causing extra CPU times. Finally, the accuracy of the results have been evaluated by showing different ignition models.

ÖZET

N-HEPTAN DETAYLI MEKANİZMASININ YÖNLENDİRİLMİS İLİŞKİLER GRAFİĞİ VE HESAPLAMALI TEKİL PERTÜRBASYON YÖNTEMLERİYLE İNDIRGENMESİ

Enerji üzerinde artan talep, bilimadamları ve mühendisleri tasarladıkları makinalarda yeni ve verimli yollar bulma konusunda heveslendirmiştir. Bu amaç uğruna, enerji sahasında ki öneminden dolayı fosil yakıtlar üzerine muazzam bir çaba gösterilmiştir. Yakıtların bilgisayarlar yardımı ile modellenmesi, ucuzluğu ve verimi sebebi ile en faydalı methodlardan biridir. Burada ki en önemli noktalardan biri de simulasyonlarda kullanılan yakıtlara ait verilerin güvenirliğidir. Bu kapsamda, yakıtları bütün türleri ve tersinir reaksiyonları dikkate alan detaylı mekanizmaların kullanarak simule edilmesi gerekmektedir. Ancak, detaylı mekanizmalar ile çalışmak detay düzeyine bağlı olarak sadece zaman kaybından başka bir şey değildir. Bu tez çalışmasında, en bilinen dizel muadili yakıtlardan biri olan, 654 molekül, ve 4866 tersinir reaksiyondan oluşan n-heptane adlı yakıt indirgenmiştir. Bu kapsamda , ilk olarak yönlendirilmiş ilişkiler grafiği metodu, n-heptanın adyabatik ateşleme için geniş aralıkta ki sıcaklık, basınç ve stokiyometri için uygulanmıştır.Sonuç olarak 135 molekül ve 1309 tersinir reaksiyondan oluşan iskelet mekanizma elde edilmiştir. Buna ek olarak, stif olan reaksiyonların elimine edilmesi amacı ile zaman analizi methodlarından biri olan hesaplamalı tekil pertürbasyon metodu kullanılmıştır. Bu şekilde, ekstra CPU zamanına sebep olan stifliği elimine edebilmek mümkün olmuştur. Son olarak, elde edilen sonuçların doğruluğu farklı ateşleme modelleri kullanılarak değerlendirilmiştir.

TABLE OF CONTENTS

LIST OF FIGURES

LIST OF TABLES

LIST OF SYMBOLS

A	Frequency factor
b^i	Basis vector
b_o^m	Refined basis vector
c_i	Molar concentration
E_A	Activation energy
F	Correction term
f_i	Amplitude
g	Main chemical vector
i	Index
j	Jacobean matrix
k_f	Rate constant for the forward reaction
k_b	Rate constant for the backward reaction
k	Reaction rate constant
k_B	Boltzman constant
m	Mass
n	Reaction order
N_{AV}	Avagadro number
Q	Projection matrix
P	Pressure
P_m	Fast reaction pointer
r_{AB}	Dependence matrix of A for B
R_A	Number of reaction
J	Jacobian matrix
K_c	Equilibrium constant based on concentration
R_u	Universal gas constant
S_A	Dependent set of A
t	Time
T	Temperature

V	Volume
W	Molecular weight
Y_i	Mass fraction
α	Stoichiometric coefficient vector
a_j	Basis vector
a_m^o	Refined basis vector
Γ_r^r	Subspace projection matrix
ε	Threshold value
Z	Molecular collision frequency per unit area
$\Theta_{m''}^m$	Refined subspace projection matrix
I	Identity matrix
λ	Lambda matrix
M	Third-body collision partner
μ	Reduced mass
$\in$	Ratio of the intrinsic time scale
δ	Kronecker delta
σ	Molecular diameter
τ	Time scale
v'	Stoichiometric coefficient for reactants
v''	Stoichiometric coefficient for products
$\overline{v}$	Maxwellian mean velocity
Φ	Equivalence ratio
X_i	Mole fraction
Ω	Net reaction rate
w	Production rate
$\hat{w}_i$	Net species volumetric production rate

LIST OF ACRONYMS/ABBREVIATIONS

CFD	Computational Fluid Dynamics
CPU	Central Processing Unit
CSP	Computational Singular Perturbation
DFS	Deep First Search
DRG	Directed Relation Graph
DRGASA	Directed Relation Graph with Aided Sensitivity Analysis
DRGEP	Directed Relation Graph with Error Propagation
DRGEPSA	Directed Relation Graph with Error Propagation and Sensitivity Analysis
DRGX	Directed Relation Graph with Expert Knowledge
HCCI	Homogeneous Charge Compression Ignition
ILDM	Intrinsic Low Dimensional Method
LOI	Level of Importance
LLNL	Lawrence Livermore National Laboratory
MW	Molecular Weight
QSSA	Ouasi Steady State Assumption
PAHs	Polycyclic Aromatic Hydrocarbons
PCAF	Principal Component Analysis of Matrix F
PE	Partial Equilibrium
PRF	Primary Reference Fuel
TRF	Three-component Toluene Reference Fuel

1. INTRODUCTION

Energy is one of the most fundamental topics of today's world and there have been conducted numerous studies in this field such as bio-fuels, clean energy application etc. Combustion has an important role since at least 75 % of energy demand is met by the combustion of fossil fuels. Moreover fossil fuels will continue to provide the world's expanding energy needs in the foreseeable future [1].

Combustion is defined as -the sequence of exothermic chemical reactions between a fuel and an oxidant mostly oxygen. As a result of these chemical reactions heat and light are released. Furthermore a very large number of different species are created and released to atmosphere as exhaust gases. Combustion stands out as the main energy source for the human kind in today's world. The original substance in combustion is called the fuel, and the source of oxygen is called the oxidizer. The fuel can be a solid, liquid, or gas. The oxidizer, likewise, could be a solid, liquid, or gas, but is usually a gas (air).

As mentioned above; during combustion, new chemical substances are created from the fuel and the oxidizer. Most of the combustion products come from chemical combinations of the fuel and oxygen. Depending on the type of fuel product gases may contain nitrogen or hydrogen in addition to carbon. Some of the combustion products created during the combustion process are pollutants. For this reason not only combustion scientists but also others who consider environment and pollution must pay great attention to combustion phenomena. Another important factor is that combustion has many applications such as;

- Propulsion
- Power Generation
- Heating Systems
- Industrial processes
- Energetic Materials

- Fire Safety
- Incineration

For combustion to occur there are three required conditions: a fuel to be burned, a source of oxygen, and a source of heat. As a result of combustion, exhausts are created and heat is released. You can control or stop the combustion process by controlling the amount of the fuel available, the amount of oxygen available, or the source of heat [2].

The various types of fuels (like liquid, solid and gaseous fuels) that are used depend on various factors such as costs, availability, storage, handling, pollution and availability of combustion equipments. The fuels used in combustion processes are mixtures of several hundred different hydrocarbons of various groups (CxHy[Oz]) These components differ with reference to molecular size and structure. As a result they sometimes have strongly varying properties. Some important fuels used in combustion processes are methane, ethane, gasoline, iso-octane, kerosene etc.

The knowledge of the fuel properties helps in selecting the right fuel for the right purpose and for the efficient use of the fuel. Laboratory tests are generally used for assessing the nature and quality of fuels.

One of the most important factors affecting combustion is the temperature. The temperature of the combustion products is high because of the heat that is released during combustion. Because of high temperature, combustion products are in gas form, but there can be liquid or solid exhaust products as well. Soot, for example, is a form of solid product that occurs in some combustion processes.

Heat is considered a very crucial for combustion processes because most combustion processes take place in order to obtain heat only. During the combustion process, as the fuel and oxidizer are turned into combustion products, heat is generated. A source of heat is also necessary to start combustion. Gasoline and air are both present in automobile fuel tank; but combustion does not occur because there is no source of heat. Since heat is both required to start combustion and is itself a product of

combustion, it can be seen why combustion takes place very rapidly. Also, once combustion gets started, it does not have to be provided the heat source because the heat of combustion will keep things going.

In the light of aforementioned topics; scientist and engineers are trying to obtain more and more efficient energy converting machines such as engines, turbines and furnaces. In order to understand these equipments and their usage one should have great knowledge on how to track physical and chemical changes in these systems.

An experimental investigation of a combustor requires expensive hardware. Also design must be rebuilt after each modification during the experiment. Numerical simulations, on the other hand, can provide more detailed information. Also one can make the modifications in geometry and operating conditions much faster and can see the difference, therefore numerical studies reduce time for design and the cost for experimental set-up. For this reason computer simulations have a great role in designing combustion equipments. Simulating combustion of large hydrocarbons is a challenging task due to stiffness and large number of differential equations. Therefore reduction of large kinetic mechanisms which is the description of what occurs in molecular level in chemical reactions plays a significant role here. As it will be mentioned in this thesis in detail, now reduction makes it possible to simulate combustion of large hydrocarbon fuels in a reasonable time.

2. COMBUSTION AND CHEMICAL KINETICS

In this chapter some important concepts related to combustion and chemical kinetics are discussed. The study of elementary reactions and their rates are called chemical kinetics and it is a specialized branch of physical chemistry. There has been tremendous work done in combustion to define the detailed reaction mechanism of combustion processes [2–5].

Two important data while defining of a mixture are the mole and mass fractions. Consider a mixture of ideal gases composed of N_1 moles of species 1, N_2 moles of species 2, etc. The mole fraction of species i, which is denoted as X_i can be calculated as:

$$X_i \equiv \frac{N_i}{\sum_{i=1}^{I} N_i} = \frac{N_i}{N_{tot}} \tag{2.1}$$

Similarly, the mass fraction of species i, which is defined as Y_i is

$$Y_i \equiv \frac{m_i}{\sum_{i=1}^{m} m_i} = \frac{m_i}{m_{tot}} \tag{2.2}$$

Also, summation of all the mass or mole fractions is unity:

$$\sum_i X_i = 1 \tag{2.3}$$

$$\sum_i Y_i = 1 \tag{2.4}$$

The mole and mass fractions can be converted from one to another via using the equations given below

$$Y_i = X_i W_i / W_{mix} \tag{2.5}$$

$$X_i = Y_i W_{mix}/W_i \tag{2.6}$$

where the W_{mix} is the mixture molecular weight and it is stated as

$$W_{mix} = \sum_i X_i W_i \tag{2.7}$$

$$W_{mix} = \frac{1}{\sum_i (Yi/W_i)} \tag{2.8}$$

From the equations above; it is possible to calculate partial pressure for a species. For ideal gases; total pressure is the sum of partial pressures of components:

$$P = \sum_i P_i \tag{2.9}$$

$$P_i = X_i P \tag{2.10}$$

2.1. Stoichiometry and Equivalence Ratio

Stoichiometry is the calculation of relative quantities of reactants and products in chemical reactions. If the quantity of the oxidizer is exactly the amount that needed to burn the quantity of the fuel completely, then this mixture is called stoichiometric mixture. If the amount of oxidizer is more than stoichiometric quantity the mixture is called a lean mixture. In reverse; if the oxidizer level is less than stoichiometric quantity the mixture is called a rich mixture.

Here, an example about how to find stoichiometric is given by a hydrocarbon ($C_x H_y$) combustion reaction with dry air (21 percent O_2 and 79 percent N_2):

$$\mathrm{C}_x\mathrm{H}_y + a(\mathrm{O}_2 + 3.76\mathrm{N}_2) \rightarrow x\mathrm{CO}_2 + (y/2)\mathrm{H}_2\mathrm{O} + 3.76a\mathrm{N}_2 \tag{2.11}$$

where

$$a = x + y/4 \tag{2.12}$$

The stoichiometric air/fuel ratio is calculated as:

$$(A/F)_{stoic} = \left(\frac{m_{air}}{m_{fuel}}\right)_{stoic} = \frac{4.76a}{1}\frac{W_{air}}{W_{fuel}} \tag{2.13}$$

Φ is defined as:

$$\Phi = \frac{(A/F)_{stoic}}{(A/F)} = \frac{(F/A)}{(F/A)_{stoic}} \tag{2.14}$$

From this definition it can be apprehended that if $\Phi > 1$ then mixture is rich, if $\Phi < 1$, then fuel is lean and if $\Phi = 1$ the mixture is a stoichiometric mixture.

2.2. Chemical Kinetics of Combustion Process

Any chemical reaction, whether of hydrolysis or combustion takes place at a definite rate and the rate relies on the conditions of the system. Some important factors here are concentration of reactants, temperature, and heat loss effects. The rate of reaction can be expressed in terms of concentration of the reactants. Only important equations and concepts are given briefly in this chapter but each of these subjects are explained in detail in references [2–5].

2.3. Reaction Rates

2.3.1. The Law of Mass Action

A single, forward chemical reaction may be represented by:

$$\sum_{i=1,N} v_i^{'} M_i \xrightarrow{k_f} \sum_{i=1,N} v_i^{''} M_i \tag{2.15}$$

The rate of change in the molar concentration c_i (moles per unit volume) of species i,

$$\frac{dc_i}{dt} = \hat{w}_i \tag{2.16}$$

is related to $\hat{w}_j$ of species j by

$$\frac{\hat{w}_i}{v_i^{''} - v_i^{'}} = \frac{\hat{w}_j}{v_j^{''} - v_j^{'}} = w \tag{2.17}$$

where w represent the reaction rate (moles per unit volume per second), subscript f means forward reaction,i and j represent species. The law of mass action states that w is proportional to the product of the concentrations of the reactants to the power of stoichiometric coefficient:

$$w = k_f(T) \prod_{i=1}^{N} c_i^{v_i^{'}} \tag{2.18}$$

2.3.2. Reversible Reactions

For every forward reaction which is defined in Equation 2.15 there can be a backward reaction:

$$\sum_{i=1,N} v_i^{''} M_i \xrightarrow{k_b} \sum_{i=1,N} v_i^{'} M_i \tag{2.19}$$

So, if there exist a forward and a backward reaction, the net reaction rate can be calculated as:

$$w_{net} = k_f \prod_{i=1}^{N} c_i^{v_i^{'}} - k_b \prod_{i=1}^{N} c_i^{v_i^{''}} \tag{2.20}$$

Here; only one of the k_f or k_b is needed. Because at equilibrium, the rate of forward reaction is balanced by the rate of backward reaction.

$$\frac{k_f}{k_b} = \prod_{i=1}^{N} c_i^{(v_i^{''} - v_i^{'})} \tag{2.21}$$

From this equation K_c is

$$\frac{k_f}{k_b} = K_c \tag{2.22}$$

At the end we can finally calculate net reaction rate as

$$w_{net} = k_f \left(\prod_{i=1}^{N} c_i^{v_i^{'}} - K_c^{-1} \prod_{i=1}^{N} c_i^{v_i^{''}} \right) \tag{2.23}$$

2.3.3. Multistep Reactions

In reality it is very rare to see the reactants collide with each other in a single step and produce the final products. Instead of this situation; there are some intermediate elementary steps which are discussed in the subsequent sections in detail. For the $_k$ th intermediate reaction:

$$\sum_{i=1,N} v_{i,k}^{'} M_i \underset{k_{k,b}}{\overset{k_{k,f}}{\rightleftharpoons}} \sum_{i=1,N} v_{i,k}^{''} M_i \tag{2.24}$$

Then, the generalized law of mass action can be defined as

$$w_k = k_{k,f} \prod_{i=1}^{N} c_i^{v_{i,k}^{'}} - k_{k,b} \prod_{i=1}^{N} c_i^{v_{i,k}^{''}} \tag{2.25}$$

such that

$$\hat{w}_i = \sum_{k=1}^{K} (v_{i,k}^{''} - v_{i,k}^{'}) w_k \tag{2.26}$$

2.4. Global Reaction Concept

An important definition here is the global reaction. This reaction is given in Equation 2.27.

$$\text{Fuel} + a\ \text{Oxidizer} \rightarrow b\ \text{Products} \tag{2.27}$$

This –global reaction mechanism- is the overall reaction of a mole of fuel with a moles of an oxidizer to form b moles of combustion products. From experimental measurements, the rate at which the fuel is consumed can be expressed as:

$$\frac{\mathrm{d}[\text{Fuel}]}{\mathrm{d}t} = -k_G(T)[\text{Fuel}]^n[\text{Oxidizer}]^m \tag{2.28}$$

The molar concentration (kmol / m^3) is defined as $[X_i]$ of the i th species in the mixture. Equation 2.28 declares that the rate of disappearance of the fuel is proportional to each the reactants raised to a power. k_G is called the global rate coefficient and in general it is a function of temperature. The minus in the right hand side of the equation states that the fuel concentration decreases. The exponents n and m are the reaction orders. That means the reaction is nth order with respect to fuel and mth order with respect to oxidizer. When it comes to reaction overall order; $(n + m)$th order. Unfortunately; global reactions are not very useful because they do not give enough information for the system. They do not provide a basis for understanding what is actually happening chemically in the system which is being investigated. In real life many intermediate species take place in the elementary reactions and their corresponding reactions which must be examined very well. The collection of elementary reactions necessary to describe an overall reaction is called a reaction mechanism. Chemical kinetics of a combustion process contains many species and reactions among these species which are not seen in the global reaction. While studying combustion these elementary reactions and species have important roles.

2.5. Elementary Reaction Rates

Elementary reactions accumulate and form complex reaction systems. The molecularity defined as the number of reactants involved in the reaction. Elementary reactions named after their molecularity. Elementary reaction can be classified into three categories. Unimolecular reactions, bimolecular reactions and trimolecular reactions.

2.5.1. Unimolecular Reactions

In this reaction type one molecule transforms itself into one or more products. Examples for this reaction type is radioactive decay, decomposition or isomerisation. Another important factor about unimolecular reaction is that they are often first-order reactions.

2.5.2. Bimolecular Reactions and Collision Theory

Most elementary reactions in combustion are bimolecular rections which means two molecules collide and react and form two products. For example,

$$\mathrm{A} + \mathrm{B} \rightarrow \mathrm{C} + \mathrm{D} \tag{2.29}$$

The rate of the reaction is proportional to the concentration (kmol / m^3) of the two reactant species:

$$\frac{\mathrm{d}[\mathrm{A}]}{\mathrm{d}t} = -k_{bimolec}[\mathrm{A}][\mathrm{B}] \tag{2.30}$$

All elementary bimolecular reactions are overall second order. $k_{bimolec}$ is a function of temperature but this time it has a theoretical basis. This theoretical basis can be gained from looking at collision theory. Actually; the collision theory has some shortcomings when it comes to the bimolecular reactions. Nonetheless; it provides a way to understand bimolecular reactions. The concept starts from collision frequency

of a pair of molecules. Consider a molecule of diameter σ traveling with constant speed υ and experiences collisions with the same diameter stationary molecules. If the stationary molecules are randomly distributed, their densities are n/V. So the number of collisions of this travelling molecule:

$$Z \equiv \text{collisions per unit time} = (n/V)\upsilon\pi\sigma^2 \tag{2.31}$$

In real life, all molecules are not stationary but moving. For this reason the Maxwellian velocity distribution is applied. Collision number becomes:

$$Z_c = \sqrt{2}(n/V)\pi\sigma^2\overline{v} \tag{2.32}$$

This equation is only valid for identical molecules. We can extend this theory for different molecules having hard sphere diameters of σ_a and σ_B:

$$Z_c = \sqrt{2}(n_B/V)\pi\sigma_{AB}^2\overline{v}_A \tag{2.33}$$

Still this equation is valid only for two molecules. We are interested in collision between all molecules:

$$Z_{AB}/V = \frac{\text{Number of collisions between all A and all B}}{\text{unit volume x unit time}} \tag{2.34}$$

$$Z_{AB}/V = (n_A/V)(n_B/V)\pi\sigma_{AB}^2(\overline{v}_A^2 + \overline{v}_B^2)^{\frac{1}{2}} \tag{2.35}$$

This equation can be expressed in terms of temperature:

$$Z_{AB}/V = (n_A/V)(n_B/V)\pi\sigma_{AB}^2\left(\frac{8k_BT}{\pi\mu}\right)^{\frac{1}{2}} \tag{2.36}$$

where k_B= Boltzman constant $= 1,381.10^{-23}$J/K, $\mu = \frac{m_A m_B}{m_A + m_B}$, T = absolute temperature (K). So, the reaction rate equation can be written for the bimolecular reaction defined

by Equation 2.29 between molecules A and B:

$$-\frac{\mathrm{d[A]}}{\mathrm{d}t} = (Z_{AB}/V)PN_{AV}^{-1} \tag{2.37}$$

N_{AV} is the Avagadro Number ($6.022x10^{26}$ molecules/kmol). The reaction rate can be expressed as product of two factors which are energy factor $exp[-E_A/R_uT]$ ((E_A) is called activation energy) and steric factor (p). Therefore, Equation 2.37 can be written as:

$$-\frac{\mathrm{d[A]}}{\mathrm{d}t} = pN_{AV}\sigma_{AB}^2\left[\frac{8\pi k_BT}{\mu}\right]^{\frac{1}{2}} exp[-E_A/R_uT][A][B] \tag{2.38}$$

From this equation $k(T)$ can be extracted as:

$$k(T) = pN_{AV}\sigma_{AB}^2\left[\frac{8\pi k_BT}{\mu}\right]^{\frac{1}{2}} exp[-E_A/R_uT] \tag{2.39}$$

Moreover, the bimolecular rate coefficient can be found from the Arrhenius form:

$$k(T) = Abexp(-E_A/R_uT) \tag{2.40}$$

Arrhenius form is an empirical form, so experimental data play important role when defining $k(T)$. The other parameters which can be found from experimental results are added to equation in order to find much more reliable results. Final equation is:

$$k(T) = AT^bexp(-E_A/R_uT) \tag{2.41}$$

A, b and $exp(-E_A/R_uT)$ are experimental data and can be found from the literature [2].

2.5.3. Trimolecular Reactions

In this reaction type three molecules are needed for collision. This type of reaction is very rare to see because three molecules must collide at the same time. Trimolecular

reactions are third order and their rates can be calculated with Equation 2.43:

$$\mathrm{A} + \mathrm{B} + \mathrm{M} \rightarrow \mathrm{C} + \mathrm{D} \tag{2.42}$$

$$\frac{\mathrm{d}[\mathrm{A}]}{\mathrm{d}t} = -k_{\mathrm{trimolecular}}[\mathrm{A}][\mathrm{B}][\mathrm{M}] \tag{2.43}$$

3. MECHANISM REDUCTION TECHNIQUES

Thanks to advancement in the chemistry, now, detailed combustion chemical mechanism of fuels are available. Multi-purpose computational fluid dynamics (CFD) codes can simulate very complex reactive flows and predict ignition time, mole fractions and emissions etc [7]. But, reduction of large kinetic mechanisms is needed. Reasons can be lined up as stiffness, cpu time and chemical understanding. Even for today's advanced computer systems it is almost impossible to simulate combustion of large hydrocarbons under turbulent flow conditions with detailed chemical kinetics models. For these reasons; reducing of large kinetic mechanism is inevitable. In the light of aforementioned problems many reduction techniques have been developed in the last decades. These techniques have many different classifications but there is no precise classification for them. Most common classification divides the techniques into two categories. First is the skeletal reduction. Second is the time scale analysis. These two classes will be examined in detail.

3.1. Skeletal Reduction

While reducing a detailed mechanism, first step is the skeletal reduction. Skeletal reduction techniques eliminate the number of species and reactions which are considered unimportant for the particular condition that is being studied [8]. After this point; the resulting mechanism called skeletal mechanism, and this mechanism is a subset of the detailed mechanism. This mechanism can be used in cfd applications or may be the subject of other reduction techniques, for further reduction. There have been tremendous works in the last decades in this field so as to develop much smaller mechanism. In literature it is easy to find variety of skeletal reduction techniques with specific pros and cons. Some techniques are just found by making some advancement in the old method. On the other hand some scientist developed new ways to reduce detailed mechanism. Finally some techniques are combination of two or three skeletal reduction methods.

Here some brief information is given about some of the most popular and basic skeletal reduction techniques.

3.1.1. Sensitivity Analysis

The oldest and the most widely used technique for the reduction of large scale kinetic mechanisms is the application of sensitivity analysis. This technique gained acceptance in the late 1980s. It has been an integral part of the analysis and reduction of detailed mechanisms since that time. Turanyi's paper is a key point in order to understand basic in sensitivity analysis [9]. Sensitivity analysis can be summarized as (i) identifying the important species, (ii) determining the necessary species through investigation of the Jacobian, and (iii) eliminating insignificant species and redundant reactions [10]. In addition to reducing the number of reactions in a given mechanism, sensitivity analysis is also used to identify the rate-limiting steps, and to understand the relative importance of each reaction in the mechanism.The example of this technique can be found in the reference [11] where sensitivity analysis were used in auto-ignition example in order to investigate important reactions in the system.

When it comes to n-heptane reduction, Maroteaux *et al.* [12] paper investigate the two stage reduction of n-heptane for the HCCI process in diesel engines. In this paper the detailed mechanisms developed by Chalmers University. In this detailed mechanism there were 57 species and 250 reactions. After applying sensitivity analysis n-heptane reduced to 61 reactions and 37 species in order to reproduce the ignition delay times and the heat release as close as possible to the detailed mechanisms. After this semi reduced mechanism sensitivity analysis and steady state approximation applied again and at the end 26 reaction step and 25 species left.

Furthermore sensitivity analysis can be used as a step for reduction with or coupled with other methods such as reaction flow analysis. There are so many methods which are combined with Sensitivity Analysis such as Directed Relation Graph with Aided Sensitivity Analysis [13]. Important factor here is that sensitivity analysis is very time consuming and must be applied as the final step in the skeletal reduction. Also,

now it can be considered as conventional method and so many developments have been made since sensitivity analyses have been released. More detailed information about this method can be seen in the references. [14, 15]

3.1.2. Necessity Analysis

This skeletal reduction technique is the combination of two methods which are sensitivity analysis and reaction flow analysis. For this reason it is important to give some basic information about reaction flow analysis. Reaction flow analysis can be divided into two major categories:

- *Integral reaction flow analysis:* Integral reaction flow analysis considers the overall formation or consumption during the combustion processes. A reaction can be considered as unnecessary for a specified case, if all entries in a row are lower than a certain limit, e.g., 1 %.
- *Local reaction flow analysis:* Local reaction flow analysis considers the formation and consumption of species locally, i.e., at specific times in time-dependent problems or at specific locations in steady processes [16].

Necessity analysis method is propoed by Soyhan *et al.* [7]. In this paper iso-octane is used and desired results are obtained. In this method reactions with high sensitivity for the targets of the mechanism are detected by sensitivity analysis. After this point the less necessary species (redundant) are eliminated according to detected targets.

For n-heptane mechanism; Thomas *et al.* [17] study is a good example of necessity analysis method on n-heptane. In this study main idea was to develop very compact sub models for the alkane low-temperature oxidation and compact oxidation models for large model fuel components, such as n-decane and n-tetradecane. The skeletal model has been derived by necessity analysis method which consists of 110 species and 1170 forward reactions. In addition to this, a compact high temperature n-heptane oxidation model is presented which comprise 196 species and 2079 irreversible reactions. The starting mechanism is reduced to 47 species from 196 species and 468 reactions.

3.1.3. Reaction Rate Analysis

This method checks the result of the error in the remaining species after elimination of a species from all its consuming reactions. If this error is small compared to some threshold value then this species is considered unimportant. This method is simple to use. However, it is time consuming due to the validation for each eliminated species.

In the paper of Jun Xi a skeletal mechanism constructed from a detailed mechanism for diesel engine simulations in order to understand anthropogenic polycyclic aromatic hydrocarbons (PAHs) emission. They used Wang and Frenklach detailed n-heptane mechanism which comprise of 572 elementary reactions and 108 species. In this reduction method they took advantage of CHEMKIN which was developed and distributed by Sandia National Laboratories. The reduced model have been obtain with 76 elementary reactions and 48 chemical species [18].

3.1.4. A Directed Path Flux Analysis

The main idea of this method is to analyze multiple path generations of each species using the formation and consumption fluxes. These are then used to identify the important reaction pathways and the associated species. In order to start a number of key species are selected and a threshold value is defined. This method has similarities with Directed Relation Graph method. An example of this method in the literature was done for n-heptane mechanism by Sun *et al.* [19]. The detailed mechanism consists of 116 species. The reduced model consists of 56 species. The pre-selected key species were n-heptane, oxygen and nitrogen. An ignition model was constructed using Chemkin codes in order to compare detailed and reduced mechanism.

3.1.5. Atomic Flux Analysis Method

Atomic flux analysis method makes an analysis of all the pathways in the reaction system according to user defined parametric conditions in order to remove inactive

species. In the literature, atomic flux analysis method has been used to obtain skeletal kerosene mechanism. The detailed mechanism was consists of 225 species and 3493 irreversible reactions. The method eliminated 91 inactive species and their 1361 corresponding reactions [20].

3.1.6. Directed Relation Graph Method

DRG is one of the most popular skeletal mechanism reduction techniques. From the beginning of its usage in reduction there has been a tremendous advancement in the method, especially by combining it with reduction metfods in order to obtain highly reduced and efficient chemical kinetics mechanisms. Examples are Direct Relation Graph with Error Propagation (DRGEP) [21, 22], Direct Relation Graph with Aided Sensitivity Analysis (DRGASA) [13], Direct Relation Graph with Error Propagation and Sensitivity Analysis (DRGEPSA) [23] and Directed Relation Graph with Expert Knowledge (DRGX) [24]. More information about these methods are available in the references. [25–29]. Since this master thesis used DRG method, much more attention is given to this method.

Skeletal reduction aims finding and eliminating unimportant reactions or species. It is much more involved to find unimportant species than unimportant reactions due to strong species coupling. The DRG method was developed to find species coupling [25]. In this method the main idea is that; species in the reactions are mapped to a graph and strongly coupled species are identified through linear-time graph searching [26]. Below, the process of DRG method is given step by step. Species couplings are identified and they are mapped to a graph.

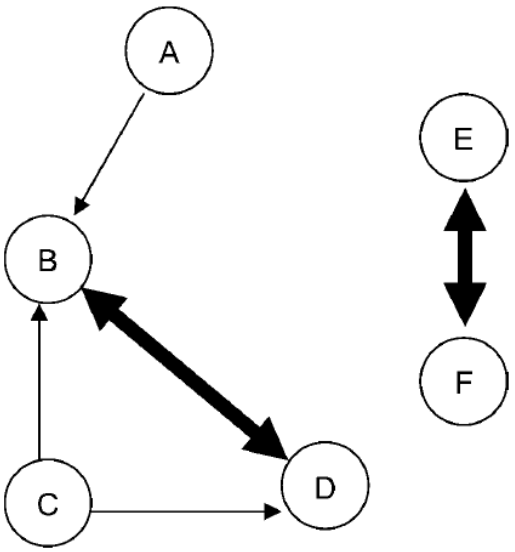

Figure 3.1. A Directed Relation graph showing species coupling.

This graph consists of nodes and vertices. Each node in the graph represents a species in the detailed mechanism and a vertex shows the dependence in between the species. In other words, if there is a vertex between two species, (for example species A and species B in the figure), and the vertex that points to B from A means removal of B causes a significant error to production rate of A. As a result; in order to find the production rate of A, B should be kept in the mechanism. The equation for the production rate of A is given in the Equation 3.1:

$$R_A = \sum_{i=1,I} v_{A,i} w_i \tag{3.1}$$

$$w_i = k_{fi} \prod_{j=1}^{K} C_j^{v''_{ij}} - k_{bi} \prod_{j=1}^{K} C_j^{v''_{ij}} \tag{3.2}$$

$$k_{fi} = [A_i T^{n_i} exp(-E_i/RT)] F_i \tag{3.3}$$

where the subscripts i and j, respectively, designate the ith elementary reaction and the jth species, $v_{A,i}$, is the stoichiometric coefficient of species A, w_i is the production rate, k_{fi} andk_{bi} are the forward and backward reaction rates, respectively, C_j is the molar concentration, $v_{ij}^{'}$ ij and $v_{ij}^{''}$ are respectively the forward and backward stoichiometric coefficients,A_i is the frequency factor, T is the temperature, E_i is the activation energy, and F_i is a correction term that includes the concentrations of the third body species, fall-off effects, and other special correction terms.

The most important factor in DRG method is to find influence of one species onto another. For this reason, the equation Equation 3.4 is used to calculate how important B when finding the production rate of A. This equation is called normalized contribution of B to the production rate of A.

$$r_{AB} = \frac{\sum_{i=1,I} |v_{A,i} w_i \delta_{Bi}|}{\sum_{i=1,I} |v_{A,i} w_i|} \tag{3.4}$$

$$\delta_{Bi} = \left\{ \begin{array}{ll} 1 & \text{if the } i \text{ th elementary reaction involves species B,} \\ 0 & \text{otherwise.} \end{array} \right\} \tag{3.5}$$

r_{AB} is a number between 1 and 0. It can be easily seen that if the normalized contribution of r_{AB} is large enough, the removal of B from skeletal mechanism cause significant error while calculating the production rate of A. As a result, if A should be kept in the skeletal mechanism, so B should be remained also. In this situation, A is said to be strongly coupled to B.

While defining dependencies of a specie to another a threshold value ε is needed. If $r_{AB} < \varepsilon$, then, the dependence is considered negligible. Thus, it can be said that there are two important rules when studying DRG:

(i) Each node in DRG is uniquely mapped to a species in the detailed mechanism.
(ii) There exists a directed edge from A to B if and only if $r_{AB} < \varepsilon$

Therefore, species A depends on species B if and only if there exists a directed path from A to B in DRG which means B is reachable from A. For each species A, there exists a group of species, which are reachable from A, and this set of species is defined as the dependent set of A, which is denoted as S_A. If A is an important species in the skeletal mechanism, its dependent set S_A should be kept with it so as to calculate its production rate correctly. Finally, for each starting species a, a deep first search (DFS) is applied to the graph to identify the dependent set S_A . After identifying the dependent set for each starting species, the species constituting the skeletal mechanism is then the union of these dependent sets. Therefore, the elementary reaction set of the skeletal mechanism can be obtained by eliminating all the elementary reactions in the detailed mechanism, which do not contain any of the species in the skeletal mechanism.

These techniques mentioned in this chapter is not exhaustive of all the methods used in the literature, but rather a sample of mostly used skeletal reduction techniques. A table is given below which lists the reduction technique, reference paper and size of obtained skeletal mechanism and size of the original detailed mechanisms. The example fuel is mostly n-heptane.

3.2. Time Scale Analysis

Skeletal mechanism contains only elementary reactions, but it can be still considered as detailed mechanism. For this reason skeletal mechanism may still be too large for demanding simulations. Furthermore numerical stiffness caused by the large range of time and length scales may be problematic [36]. The most widely accepted solution to stiffness problem is the simplification of the detailed mechanism, in this case the skeletal mechanism, by applying some mathematical tools. This mathematical simplification is based on partial equilibrium and quasi steady state assumptions. The methods based on these two assumptions have been widely used for decades. Time scale analysis methods are the ancestors of reduction techniques, because before skeletal reduction techniques, simplifications were made by QSSA and partial equilibrium techniques. These techniques mostly do not eliminate redundant species, instead they

remove stiffness.

3.2.1. Quasi Steady State Assumption

During combustion, highly reactive intermediate species are formed in the process such as radicals. The detailed mechanism can be simplified by applying steady-state approximation to these reactive species. Quasi-steady state occurs when the production and destruction rates of a particular species are in approximate balance. This is because, after a rapid initial buildup in concentration, radicals are destroyed at the same time while they are formed. As a result; the concentration of radicals are very small compare to the concentration of the reactants or products [2].

3.2.2. Partial Equilibrium

Partial equilibrium can be shortly defined as the approximate balance between the forward and reverse reaction rates of a single or a group of fast reactions [34]. In combustion processes slow and fast reactions occur simultaneously but the fast reactions are rapid in both the forward and reverse directions. These fast reactions are usually chain-propagating or chain-branching reactions. In this situation it is possible to think that these fast reactions are equilibrated. Therefore, this simplifies the chemical kinetics [2]. There are many examples in literature that employs partial equilibrium assumption in order to simplify detailed mechanism.

Partial equilibrium and steady-state assumptions are the oldest reduction techniques in chemistry and main disadvantage of these two techniques is that they rely on experience and intuition of the user. In the light of these two theories, there have been constructed some life time analysis methods which employ these techniques in order to get rid of stiffness. These are in general called time scale analysis. Some important examples of these methods are; Intrinsic Low Dimensional Manifold (ILDM), Computational Singular Perturbation (CSP) and Level of Importance (LOI). Each of these methods are based on partial equilibrium or quasi steady state approximation. Since; in our cases CSP method is employed, this method will be discussed in detail.

3.3. Computational Singular Perturbation Method

The CSP method was first submitted bay Lam in 1994. [37].This method mainly aims reducing the stiffness using some mathematical tools without having chemical knowledge. This method enables engineers and scientists from different areas to discard stiffness in their combustion problems without using partial equilibrium or quasi steady state assumption.

Main idea in this method is to define problem vector with different basis vectors.That vector, at the end, achieves seperating fast and slow reactions.These basis vectors must be chosen correctly. For this reason method gives some hints in order to choose correct basis vectors.Detailed mathematical model is given below how to choose basis vectors and their calculations. [37]

3.3.1. The mathematical problem

In the problem the total number of unknowns is N. This number contains all the data about the problem including concentration of the species, temperature and pressure. This y vector can be constructed as a column vector;

$$y = [y^1, y^2, ..., y^N]^T \tag{3.6}$$

The governing equation of the system is

$$\frac{d\mathrm{y}}{dt} = g(y) \tag{3.7}$$

where g is the sum of the contribution of the R elementary reactions:

$$g \equiv \sum_{r=1}^{R} s_r \Omega^r(y) \tag{3.8}$$

s_r is the stoichiometric vector and Ω^r(y) is the reaction rate of the r-th elementary reaction. The value of R is not equal to N. It can be greater or less than N

3.3.2. Basis Vectors

As it was described above g contains all the data of the problem. Since an N-dimensional vector may be expressed in terms of any set of N linearly independent basis vectors; in order to express g, a set of basis vectors are employed. $a_i(t), i = 1, 2, ..., N$ is assumed to be a set of N linearly independent column basis vectors. The inverse of this vectors can be calculated and labeled as $b^i(t), i = 1, 2, ..., N$. These vectors are row basis and their vectors dot product with coulumn basis vectors, $\odot$, gives the identity matrix.

$$\mathrm{b}^i \odot \mathrm{a}_j = \delta^i_j \qquad i, j = 1, 2, ..., N \tag{3.9}$$

g can be expressed using the basis vectors:

$$g = \sum_{i=1}^{N} a_i f^i \tag{3.10}$$

where

$$f^i \equiv b^i \odot g = \sum_{r=1}^{R} B^i_r F^r \qquad i = 1, 2, ..., N \tag{3.11}$$

$$B^i_r \equiv b^i \odot s_r \tag{3.12}$$

f^i is called the amplitude and $a_i$represent the direction of the i-th mode.

3.3.3. The Speed Ranking of the Modes

In order to find out the influence of basis vectors on the time evolution of f^i, we differentiate the equation Equation 3.11 with respect to time

$$\frac{df^i}{dt} = \sum_{j=1}^{N} \lambda_j^i f_j, \qquad i = 1, 2, ..., N \tag{3.13}$$

where

$$\lambda_j^i \equiv [\frac{d\mathrm{b}^i}{dt} + \mathrm{b}^i \odot \mathrm{J}] \odot \mathrm{a}_j, \qquad i = 1, 2, ..., N \tag{3.14}$$

$$J \equiv \frac{\partial g}{\partial y} \qquad \text{N x N Jacobian matrix} \tag{3.15}$$

It can be understood from the equation Equation 3.13 that f^i is controlled by λ_j^i. Moreover λ_j^i depends on basis vectors. If λ_j^i is diagonal, then all the modes are coupled easily but generally the non-linear nature of the problem does not let this happen. For this reason λ_j^i is generally not constant. In this theory reciprocal of an eigenvalue will be called time scale and it has the dimension of time which will be denoted as τ. If we order them in ascending values:

$$\mid \tau(1) \mid < ... < \mid \tau(i) \mid < ... < \mid \tau(N) \mid \tag{3.16}$$

3.3.4. The CSP Refinement Strategy

The CSP theory uses the ratio in order to separate fast and slow modes.

$$\in_M (t) = \left| \frac{\tau(M)}{\tau(M+1)} \right| \tag{3.17}$$

Each refinement procedure depresses the magnitude of the off-diagonal terms of λ_j^i by $O(\in_M)$.

3.3.5. The CSP Refinement Procedure

It is assumed that any moment in time, the current value of M and a set of trial basis vectors are known:

$$a_m, b^m, \qquad m = 1, 2, ..., M \tag{3.18}$$

If we compute the upper-left block of λ_j^i which is denoted here as w_n^m:

$$w_n^m \equiv \lambda_n^m = (\frac{d\mathrm{b}^m}{dt} + \mathrm{b}^m \odot \mathrm{J} \odot \mathrm{a}_n), \qquad m, n = 1, 2, ..., M \tag{3.19}$$

The inverse of w_n^m is denoted as τ_n^m

$$\sum_{n'=1}^{M} w_{n'}^m \tau_n^{n'} = \sum_{n'=1}^{M} \tau_{n'}^m w_n^{n'} = \delta_n^m, \qquad m, n = 1, 2, ..., M \tag{3.20}$$

After refinement procedure in order to separate refined basis vectors from unrefined ones those which are refined will be denoted by a superscript or subscript o.

To refine b^m row vectors,

$$b_o^m = \sum_{n=1}^{M} \tau_n^m (\frac{d\mathrm{b}^n}{dt} + \mathrm{b}^n \odot \mathrm{J}), \qquad m = 1, 2, ..., M \tag{3.21}$$

$$a_m : \text{unchanged}, \qquad m = 1, 2, ..., M \tag{3.22}$$

This step depresses the upper-right $M\mathrm{x}(N - M)$ block of λ_j^i. this step makes the fast modes purer.

To refine a_m column vectors

$$b_o^m : \text{unchanged}, \qquad m = 1, 2, ..., M \tag{3.23}$$

$$a_m^o = \sum_{n=1}^{M} (-\frac{d\mathrm{a}_n}{dt} + \mathrm{J} \odot a_n)\tau_{m,o}^n \tag{3.24}$$

This step depresses the lower-left $(N - M)$xM block of λ_j^i. This step makes the slow modes purer.

3.3.6. The Fast Subspace Projection Matrix

A Q(M) matrix can be obtained by applying

$$Q(M) \equiv \sum_{m=1}^{M} a_m b^m \tag{3.25}$$

Here this matrix will be used to separate the g vector to its fast and slow components with the help of refined basis vectors.

Also Q(M) can be written as the sum of its components:

$$Q_o^o(M) = \sum_{m=1}^{N} Q_{m,o}^o \tag{3.26}$$

If we use the refined basis vectors:

$$Q(M)_{m,o}^o \equiv a_m^o b_o^m, \qquad m = 1, 2, ..., M \tag{3.27}$$

$Q(M)_{m,o}^o$ is $m - th$ fast mode projection matrix.

$$Q_m(i) \equiv \text{the i-th diagonal element of } Q_{m,o}^o, \qquad i = 1, 2, ..., N \tag{3.28}$$

$Q_m(i)$is dimensionless and the summation of all of its components is unity. If the $Q_m(k)$ is not a small number, then species k is a CSP radical.

The fast reaction pointer of the m-th mode which is denoted as $P_m(r)$ can be calculated as

$$P_m(r) \equiv (s_r)^{-1} \odot Q^o_{m,o} \odot s_r \qquad r = 1, 2, ..., R \tag{3.29}$$

Whenever $P_m(r)$ is not a small number, the r-th reaction can be said fast reaction.

3.3.7. The Amplitudes of the Fast Modes

The original system can be divided into its slow and fast components using $Q(M)$:

$$\frac{dy}{dt} = g^{fast}(M) + g^{slow}(M) \tag{3.30}$$

where

$$g^{fast}(M) \equiv Q(M) \odot g \tag{3.31}$$

$$= \sum_{r=1}^{R} a_m f^m \tag{3.32}$$

$$f^m = b^m \odot g \tag{3.33}$$

$$g^{slow}(M) \equiv (I - Q(M)) \odot g \tag{3.34}$$

From Equation 3.13:

$$\frac{df^m}{dt} = (\frac{d\mathrm{b}^m}{dt} + \mathrm{b}^m \odot \mathrm{J}) \odot (g^{fast}(M) + g^{slow}(M)) \tag{3.35}$$

At the end of some calculations using the above equations Equation 3.34 can be written as

$$\frac{df^m}{dt} = \sum_{n=1}^{M} w_n^m (f^n - f_\infty), \qquad m = 1, 2, ..., M \tag{3.36}$$

where

$$f_\infty^m \equiv (b^m - b_o^m) \odot g, \qquad m = 1, 2, ..., M \tag{3.37}$$

If we use the refined basis vectors:

$$f_o^m \equiv b_o^m \odot g = f^m - f_\infty^m, \qquad m = 1, 2, ..., M \tag{3.38}$$

The governing equation for f_o^m is

$$\frac{df_o^m}{dt} = \sum_{n=1}^{M} w_n^m (f_o^n - \sum_{n'=1}^{M} \tau_{n'}^n \frac{df_\infty^{n'}}{dt}), \qquad m = 1, 2, ..., M, \tag{3.39}$$

From this equation it can be concluded that for large time:

$$f_o^m \to \sum_{n'=1}^{M} \tau_{n'}^m \frac{df_\infty^{n'}}{dt} \tag{3.40}$$

3.3.8. The Simplified Model

After calculating the refined basis vector, it is no more a problem to find simplified model. For this purpose $g_o^{o,fast}$ is neglected:

$$\frac{dy}{dt} \approx g_o^{o,slow} \tag{3.41}$$

where

$$g_o^{o,slow} = \sum_{r=1}^{R} s_{o,r}^{o,slow} \Omega^r \tag{3.42}$$

$$s_{o,r}^{o,slow} = (I - Q_o^o(M)) \odot s_r \tag{3.43}$$

3.3.9. The Radical Correction

For each step in refinement procedure new initial condition must be derived.This can be done using radical correction:

$$(\Delta y)_{rc} = - \sum_{m,n=1}^{M} [a_m \tau_n^m(M)(f^n - f_\infty^n)]_{t=0} \tag{3.44}$$

Computational singular perturbation method aims translating classical perturbation methods into programmable algorithms. For this reason; model reduction methods are being developed day by day. Computational singular perturbation method, also, have been studied and finally some modifications have been made on it. In the new paper of Lam [38]; it is no more needed to refine basis vector. Purpose is to find good quality basis vector which leads to separate first and slow vectors for g(y). Here basis vectors can be found analytically. One of the main advantage of the developed model is the τ which is the intrinsic time scale which can be programmable. Also it can be found for

every elementary reaction.

$$\tau^r = \left[\frac{\partial \Omega^r}{\partial y} \odot \alpha_r\right] \tag{3.45}$$

The path for CSP with new method is given below with the algorithm below. This algorithm also cantains the equations those are not given above.

3.3.10. Algorithm for CSP

(i) Calculation of s_r which are the stoichiometric coefficients of species in each reactions.These are taken from g:
$g \equiv \sum_{r=1}^{R} s_r \Omega^r(y)$

(ii) Main CSP calculation starts by defining $y_i(t)$ i=1:R.

(iii) Calculation of $\frac{\partial \Omega^r}{\partial y_i}$: r=1:R, i=1:N.

(iv) Calculation of τ^r:
$\tau^r = \left[\frac{\partial \Omega^r}{\partial y} \odot \alpha_r\right]$

(v) Sorting reactions with respect to τ^r.

(vi) Chosing of M by looking at $\frac{\tau^i}{\tau^{i+1}}$.

(vii) Calculation of β:
$\beta^r(y) = \tau^r \frac{\partial \omega^r}{\partial y}$

(viii) Calculation of $\Gamma^r_{r'}$:
$\Gamma^r_{r'} = \beta^r \odot \alpha_{r'}$

(ix) Calculation of $\Theta^m_{m''}(y)$:
$\Theta^m_{m''}(y) = \left[\Gamma^{m''}_m(y)\right]^{-1}$: m, m''=1:M.

(x) Calculation of $\tau^m_{m'}$:
$\tau^m_{m'} = \Theta^m_{m''} \tau^{m'}$

(xi) Calculation of Ω^m_∞:
$\Omega^m_\infty = -\sum_{n=M+1}^{R} \left(\sum_{m'}^{M} \Theta^m_{m''} \Gamma^{m''}_m\right) \Omega^n$

(xii) Calculation of f^m:
$f^m = \sum_{m'=1}^{M} \tau^m_{m'} \frac{\partial \Omega'}{\partial t}$
f^m must be $\ll \Omega^m_\infty$. If this condition is not satisfied, it must be repeated from

step 6 by increasing M amount of 1.

(xiii) Calculation of g^{fast}:

$g^{fast} = \sum_{m=1}^{M} \alpha_m \left[\Omega^m - \Omega_\infty^m\right]$

$g^{fast} = \sum_{m,m'=1}^{M} \alpha_m \tau_{m'}^m \frac{\partial \Omega'}{\partial t}$

(xiv) Calculation of g^{slow}:

$g^{slow} = \sum_{m=1}^{M} \alpha_m \Omega_\infty^m + \sum_{n=M+1}^{R} \alpha_n \Omega^n$

(xv) Solving $y(t + \Delta t)$ via explicit integration:

$\frac{dy}{dt} = g^{fast} + g^{slow}$

$\frac{y(t+\Delta t) - y(t)}{\Delta t} = g^{fast} + g^{slow}$

Table 3.1. Skeletal Mechanism Results of Some Important Methods and Fuels.

			Detailed		**Skeletal**	
Ref	**Fuel**	**Method**	**Species**	**Reactions**	**Species**	**Reactions**
[12]	n-heptane	Sensitivity Analysis	57	250	37	61
		Quasi Steady State Analysis	37	61	25	26
[17]	n-heptane	Necessity Analysis	196	2079	110	1170
[18]	n-heptane	Reaction Rate Analysis	108	572	48	76
[19]	n-heptane	A Directed Path Flux Analysis	116	——-	56	——-
[20]	kerosene	Atomic Flux Analysis	225	983493	134	2130
		Principal Component Analysis	134	2130	134	1220
[7]	iso-octane	Necessity Analysis	857	7193	385	——-
[15]	propane	Principal Component & Reaction Rate Analysis	36	98	13	38
[30]	bio-diesel	DRG and lumping	3299	10806	115	460
[31]	GRI3.0	PCAF and CSP	——-	124	——-	9
[32]	iso-octane	DRG and CSP	850	7212	195	802
[27]	n-heptane	DRG, isomer lumping and QSSA	561	2539	55	51
[33]	TRF mixture	DRGEPSA	1389	5935	386	1591
[23]	n-decane	DRGEPSA	2115	8157	202	846
[34]	Methylbutanoate n-heptane mixture	Sensitivity Analysis	661	3019	145	869
[35]	Biomass volatile	Reaction flow and Sensitivity Analysis	81	1403	26	91
[25]	n-heptane	DRG	561	2539	188	842
[25]	iso-ocatane		857	3606	233	959
[22]	n-heptane and iso_octane(PRF)	DRGEP	990	8476	374	1772
[13]	1,3-Butadiene	DRG and Sensitivity Analysis	94	614	46	297

4. VERIFICATION

Lu and Law paper was selected in our case in order to understand the DRG mechanism and verification of the accuracy of our system. For this reason same problem was employed which was examined in the reference paper. Firstly, reaction mechanism for C_2H_4 (ethylene) was founded from Lawrence Livermore National Laboratory(LLNL). [39] Here detailed mechanisms are available for different fuels. Data for these fuels are written in Chemkin format. These data contain three important sections. First an input file. In this file all the species names and all the reactions in terms of forward and backward are available. Secondly, all the thermodynamics data are given which are necessary for the selected fuel 'n a folder. Finally, transport property data in the final folder. This mechanism, also, can be taken from any other source. Also it is possible to create one own reaction mechanism using appropriate software but it is easy to find reliable and up-to-date reaction models. Second step is to convert this input files into compatible format for our program. Since cantera program has been employed in our system. C_2H_4 consists of 70 species and 463 elementary reactions which are same with the reference paper. Auto-ignition problem is solved for homogenous reaction system. For these calculations P,T,ϕ are selected as parameters. Chosen value of the parameters are listed below. For temperature; 1000 ,1100, 1200, 1300, 1400, 1500, 1600, 1700, and 1800 Kelvin Pressure; 0.1, 0.2, 0.3, 0.5, 0.7, 1.0, 2.0, 3.0, 5.0, 7.0, 10, 15, 20, 25, and 30 atm Equivalence ratio; 0.7, 0.8, 0.9, 1.0, 1.1, 1.2, and 1.3 We have temperature ranging from 1000 to 1800 Kelvin, pressure changes from 0.1 atm to 30 atm and ϕ starts from 0.7 and goes up to 1.3. Auto-ignition problem is solved for 945 different cases were calculated. All the data are available for combustion in these cases in example temperature variation during the ignition, mass fraction at each point, ignition delay time etc. Other step is to choose sample points from these ignition samples. First point was chosen as the beginning of ignition in order to understand characteristic of species and second point was chosen after reaching the peak temperature. For 945 cases; we ended up with 1080 points. In the reference papers it has been clarified that only 100 points are enough. Now, DRG can be applied to these points. Each point is brought to program again. This point temperature, pressure,

equivalence ratio and mole fractions are preserved. These variables are applied to fuel and DRG equation which is given in Equation 2.18 is used. r_{AB} is a 70x70 square matrix since this matrix shows the dependencies of all species in the reaction system for each species. 1080 square matrix are developed for each point. Diagonal of this matrix consists of 1's, since each species dependency on itself is one. It can be easily seen in the formulation to. At the end unimportant species can be determined using the Deep First Search (DFS) for different threshold values in this matrices. In order to apply DFS matrix must be sparse matrix in matlab program. Here our target species is C_2H_4. Different skeletal mechanisms are found from 1 to 0. These results can be found in the graph below. 5.27.

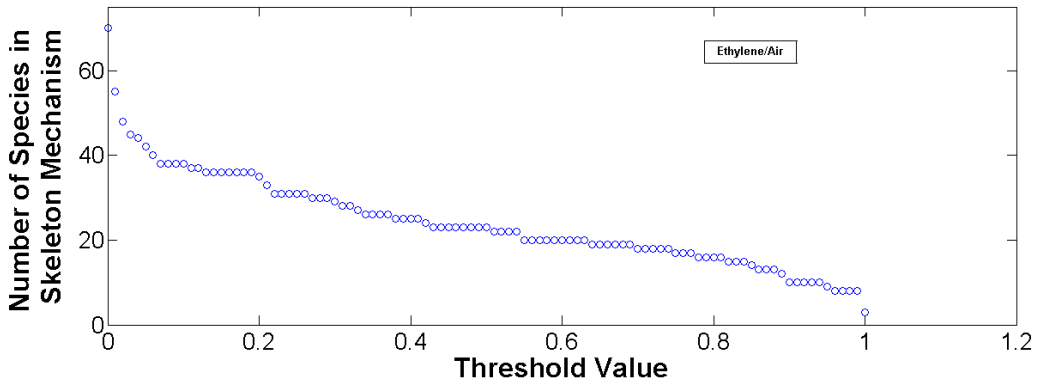

Figure 4.1. Number of species left in the skeletal mechanism according to threshold value.

As it can be seen from the graphic, when the threshold value came close to 1 skeletal mechanism contains less species. At the end only left with one species C_2H_4. Important point is to be careful about jumping point. Since these points show strong dependency on species, the selected mechanism must be chosen before or after jump due to strong couplings between species. In the light of this information; 0.13 threshold value is chosen to construct our skeletal mechanism which is the same in the reference paper. This skeletal mechanism consists of 36 species. After finding the 36 species, new code was written in order to generate new cti file which will be used in cantera program. After constructing the file 215 elementary reactions left when we ignore the

species which are beyond the directed relation. This new skeletal mechanism must be tested so as to learn that it can mimic the detailed mechanism well or not. For this reason ignition problem was chosen as it was before in the detailed mechanism and compared with different cases. Below these results are shown:

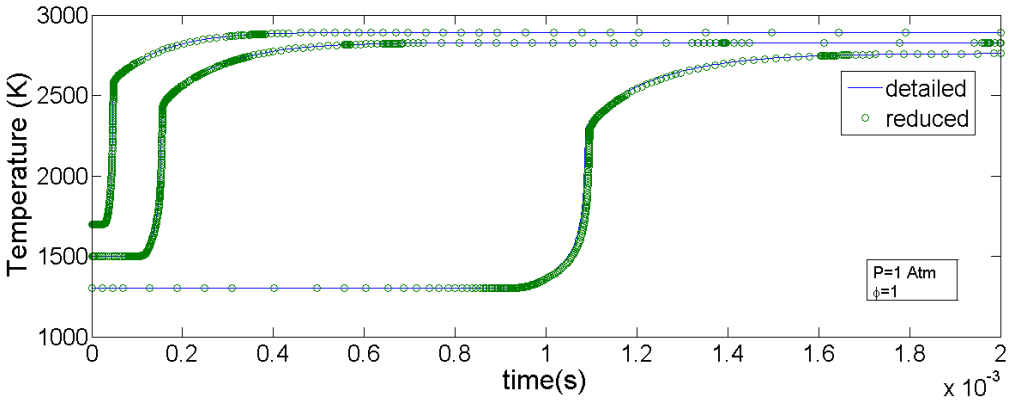

Figure 4.2. Comparison of deteailed and reduced mechanism for different initial temperatures for 1 atm and Φ=1.

As it can be understood from this graphic our skeletal mechanism can mimic the detailed mechanism well in the path of ignition for different initial temperatures.

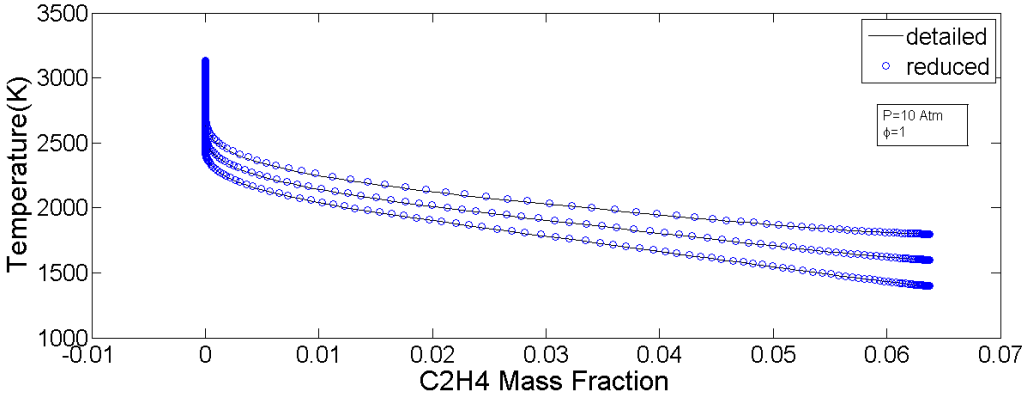

Figure 4.3. Comparision of deteailed and reduced mechanism for Temperature to C2H4 mass fraction for 10 atm and Φ=1.

After these ignition paths and mass fraction another deep investigation were made on ignition delay times for different pressures and different stoichiometric coefficients for different temperatures.

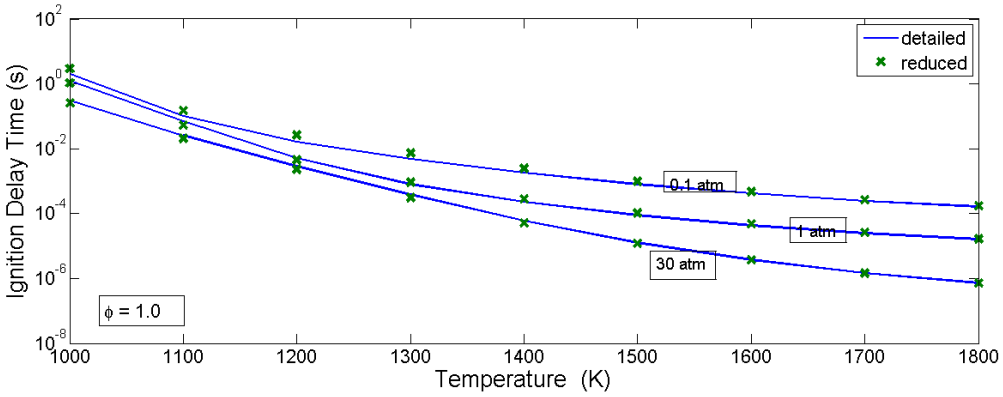

Figure 4.4. Ignition Delay Times for $\Phi = 1$.

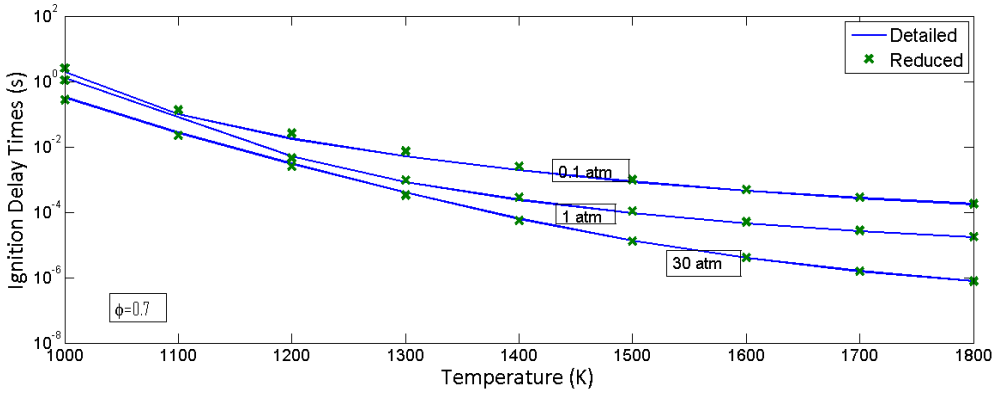

Figure 4.5. Ignition Delay Times for $\Phi = 0.7$.

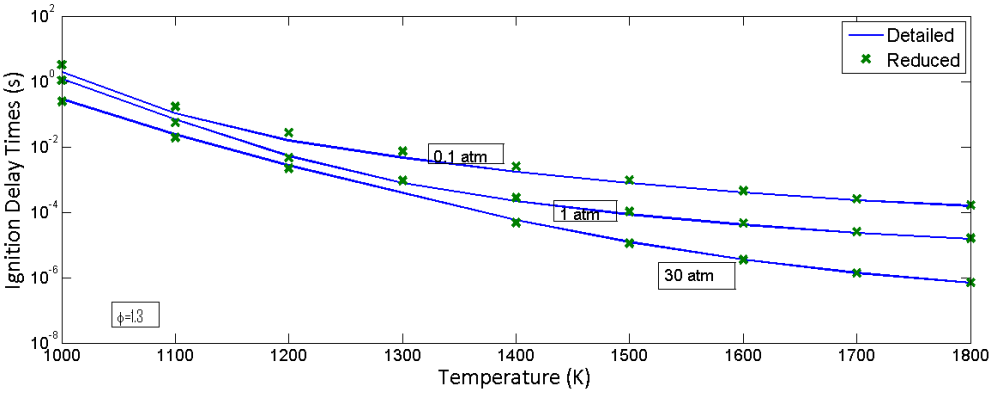

Figure 4.6. Ignition Delay Times for $\Phi = 1.3$.

As it can be understood from graphics our skeletal mechanism performs well under different conditions. It can mimic ignition delay times, mass and mole fractions correctly. After this point it is possible to apply this DRG mechanism into our main problem which is N-heptane in order to obtain skeletal mechanism.

5. SKELETAL REDUCTION OF N-HEPTANE

Detailed N-heptane mechanism was obtained from LLNL. This detailed mechanism contains all the data in terms of chemical, kinetic and thermodynamic. Same procedure is applied to N-heptane mechanism which was used in ethylene in order to convert this mechanism to cantera format. N-heptane mechanism consists of 654 species and 4846 reactions. Main path while reducing the detailed mechanim is shown in the figure below;

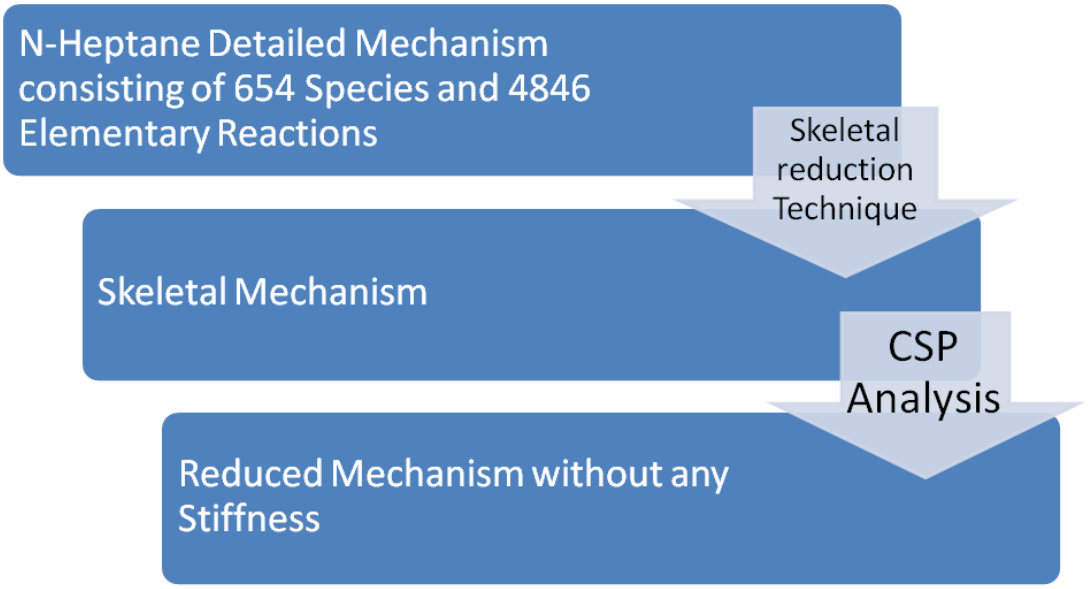

Figure 5.1. Reduction algorithm of detailed N-Heptane mechanism.

After obtaining the cantera format of n-heptane, DRG has been applied to n-heptane mechanism for different threshold values. Here again, temperatures ranges from 1000 to 1800 K. Equivalence ratio starts from 0.7 to 1.3 and pressure changes from 0.1 up to 30 atm. These ranges cover most of the ignition data. All the points

have been calculated for adiabatic ignition problem. After obtaining the results some sample points were chosen from all the results and DRG applied.All DRG results for all threshold values are given below.

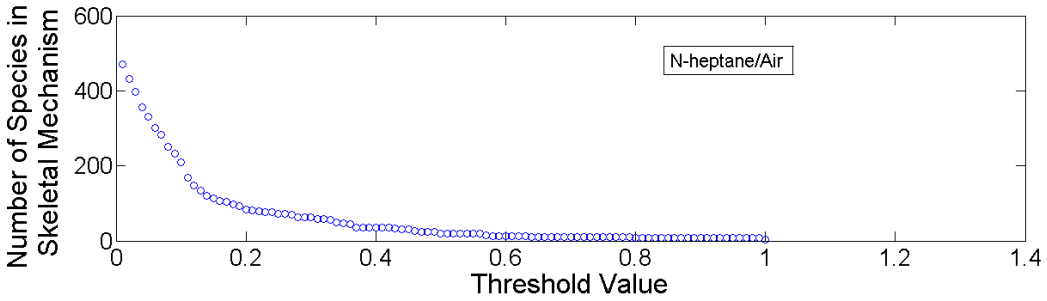

Figure 5.2. Number of species left in the skeletal mechanism according to threshold value.

Table 5.1. Skeletal mechanisms according to threshold value differences.

Threshold Value	**Number of Species in the Skeletal Mechanism**	**Number of Reactions in the Skeletal Mechanism**
1	1	-
0.75	10	33
0.50	20	54
0.28	64	583
0.25	73	697
0.20	84	842
0.13	135	1309
0.10	210	2042
0.01	608	4732
0	654	4846

Now, it is available to find different skeletal mechanisms according to different threshold values. When the threshold value comes close to 1 smaller mechanisms are available but, their accuracy is suspicious. Important point is to chose best skeletal mechanism which compromise smaller number of species and reactions, on the other

hand that mechanism must mimic the reaction system well. In ethylene case 0.13 was good choice. Here, some skeletal mechanisms were tested and the correct skeletal mechanism was chosen. Below; results are shown for different skeletal mechanisms. In these graphics 3 different skeletal mechanisms are displayed in the same graphics in order to understand which one mimic the detailed mechanism well.

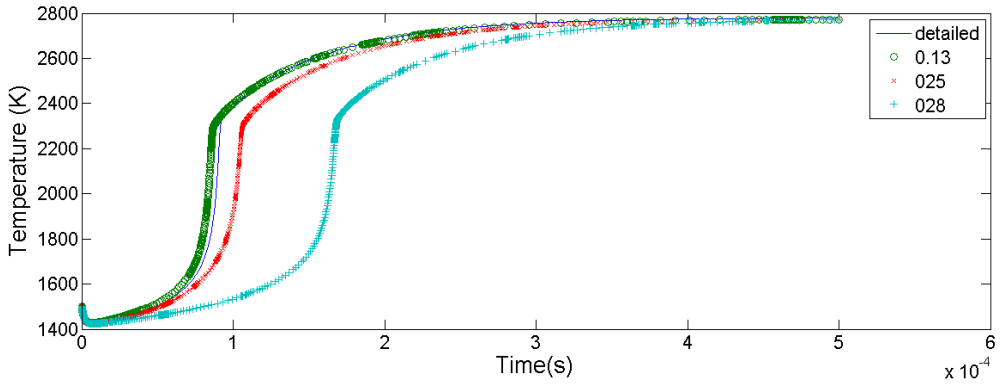

Figure 5.3. Adiabatic constant pressure ignition results of different skeletal mechanisms for 1500 K starting temperatures.

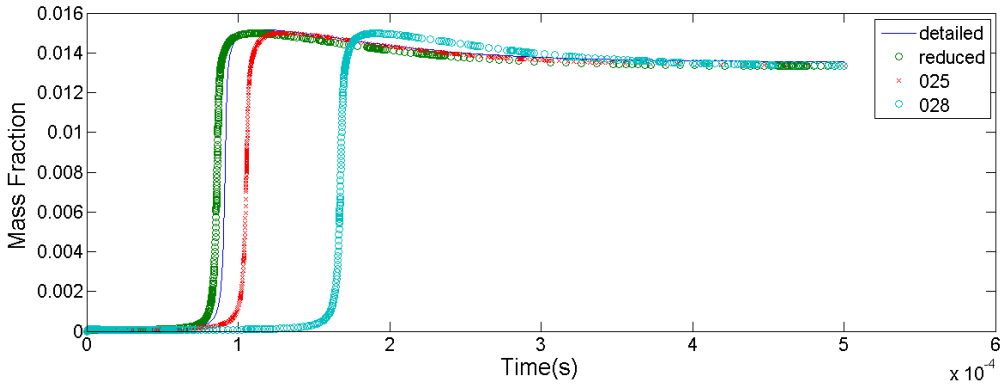

Figure 5.4. OH mass fractions for adiabatic ignition results for different skeletal mechanisms for 1500 K starting temperature.

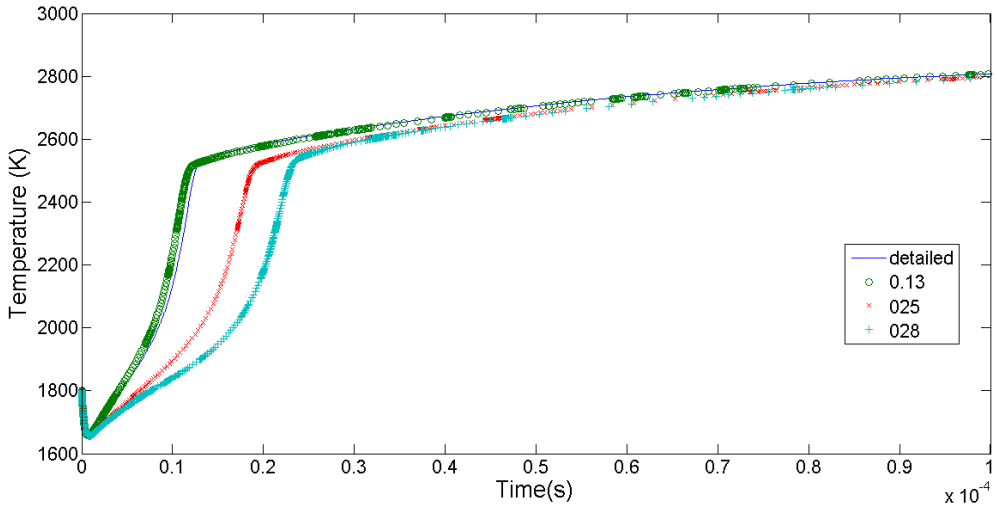

Figure 5.5. Adiabatic ignition results for different skeletal mechanisms for 1800 K starting temperature.

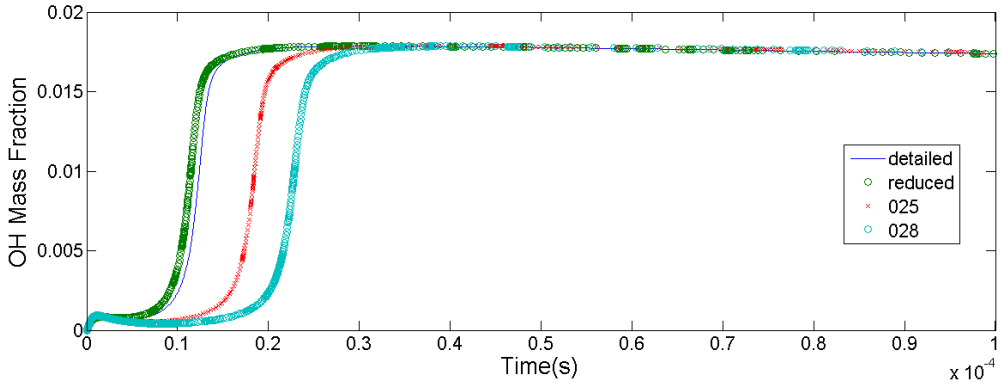

Figure 5.6. Adiabatic ignition results for different skeletal mechanisms for 1800 K starting temperature.

As it can be understood from these graphics skeletal mechanism which has the 0.13 threshold value mimics the detailed mechanism well as expected. Because a small threshold value means that skeletal mechanism gets closer to detailed mechanism. For different purposes other skeletal mechanism can be chosen with different accuracy results. Here 0.13 threshold value is a good choice because the results are almost the

same, on the other hand species number and reaction number is very few compare to detailed mechanism. For 0.13 threshold value much more results are shown below for different pressure and stoichiometric parameters. Here, temperature results and mass fractions of different species are displayed and compared. For $\Phi = 1$;

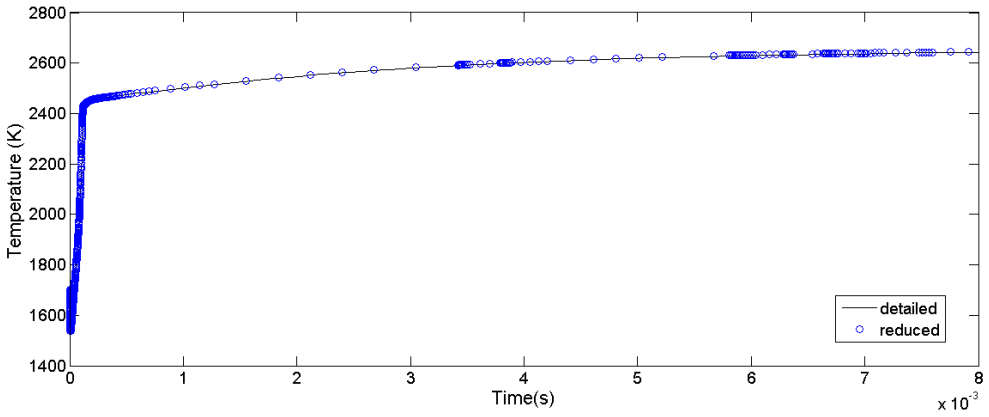

Figure 5.7. Adiabatic, constant pressure ignition result for 1700 K starting temperature at 0.1 atm.

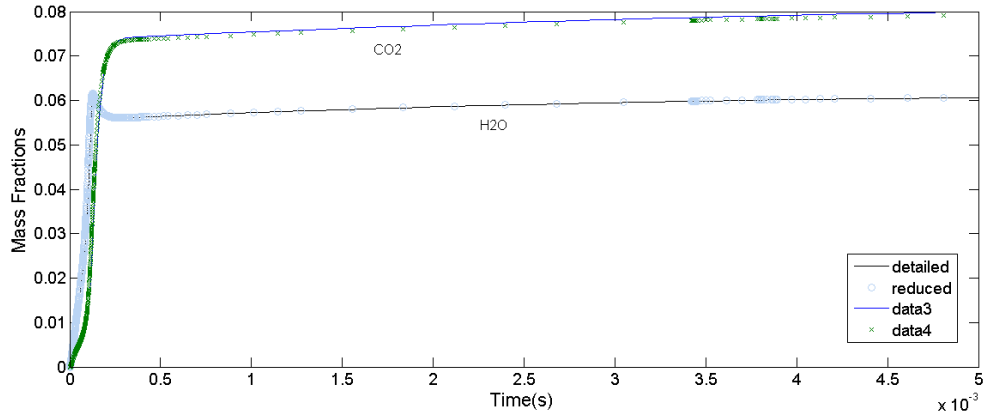

Figure 5.8. CO_2 and H_2O mass fractions at 0.1 atm for 1700 K starting temperature ignition.

Figure 5.7 and Figure 5.8 represent the ignition results for 1700 K starting temperature. As it can be understood from the results, skeletal mechanism can predict the

ignition as good as detailed mechanism in terms of temperature and mass fractions. Detailed mechanism cpu time, in this calculation, is 1046.5. On the other hand for skeletal mechanism cpu time is only 20.1 s.

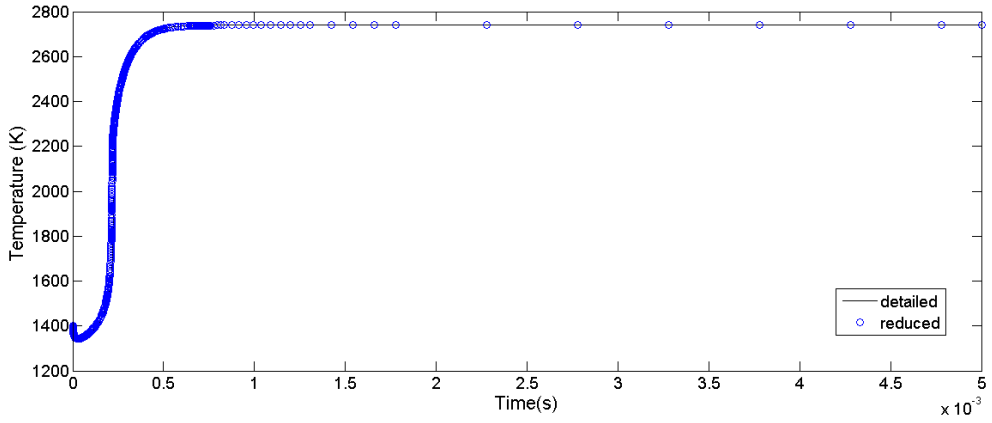

Figure 5.9. Adiabatic, constant pressure ignition result for 1400 K starting temperature at 1 atm.

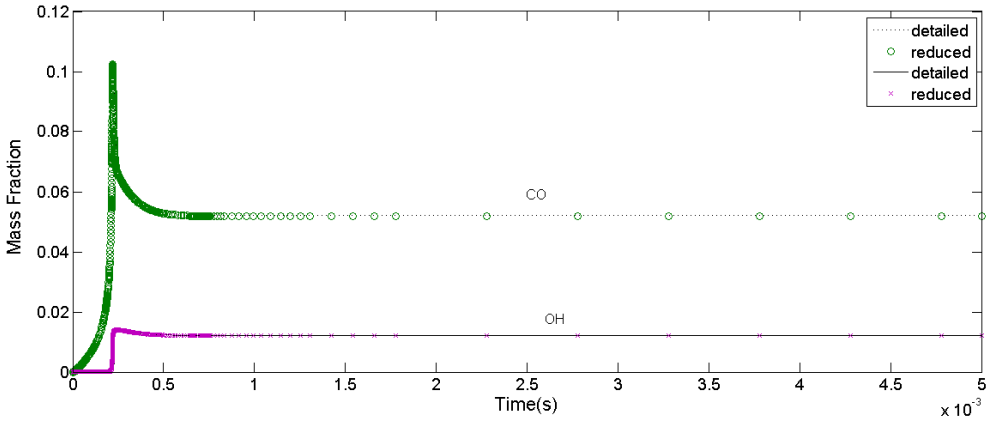

Figure 5.10. CO and OH mass fractions at 1 atm for 1400 K starting temperature ignition.

Figure 5.9 and Figure 5.10 are again for adiabatic, constant pressure ignition results with different temperature and pressure. Here the cpu times for detailed mechanism is 522.4 and for the skeletal mechanism is 14.2 s.

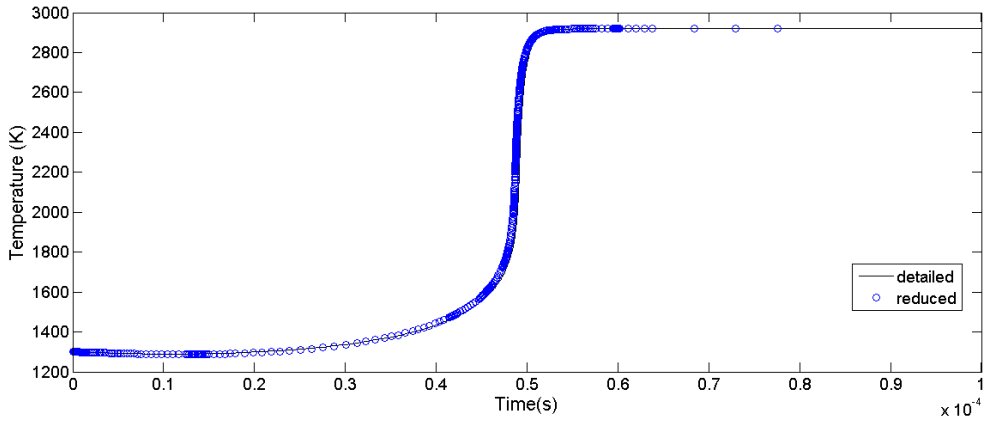

Figure 5.11. Adiabatic, constant pressure ignition result for 1300 K starting temperature at 30 atm.

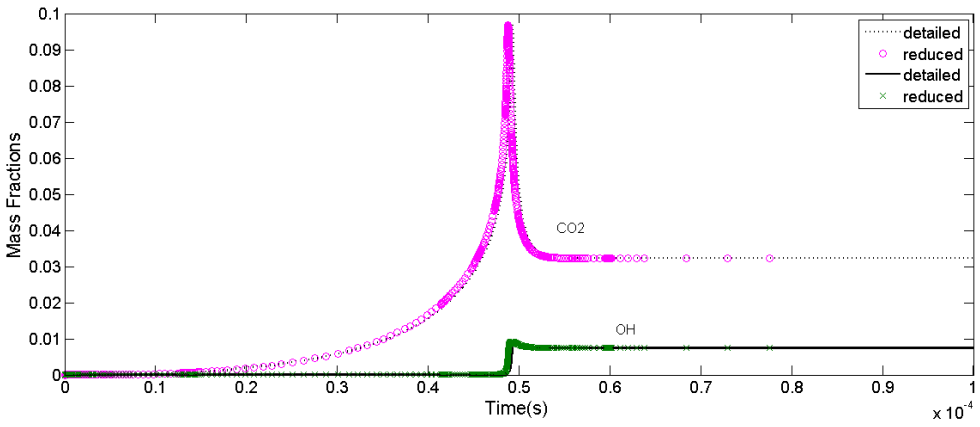

Figure 5.12. CO_2 and H_2O mass fractions at 30 atm for 1300 K starting temperature ignition.

Figure 5.11 and Figure 5.12 are the results of calculation of adiabatic, constant pressure ignition results. Cpu time of detailed mechanism is 386.4 and for the skeletal mechanism is 11.9 s. For $\Phi = 1.3$:

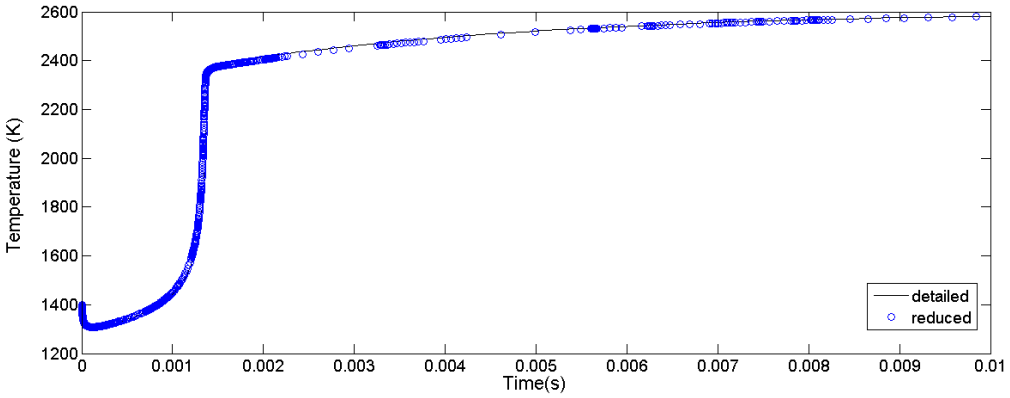

Figure 5.13. Adiabatic, constant pressure ignition result for 1400 K starting temperature at 0.1 atm.

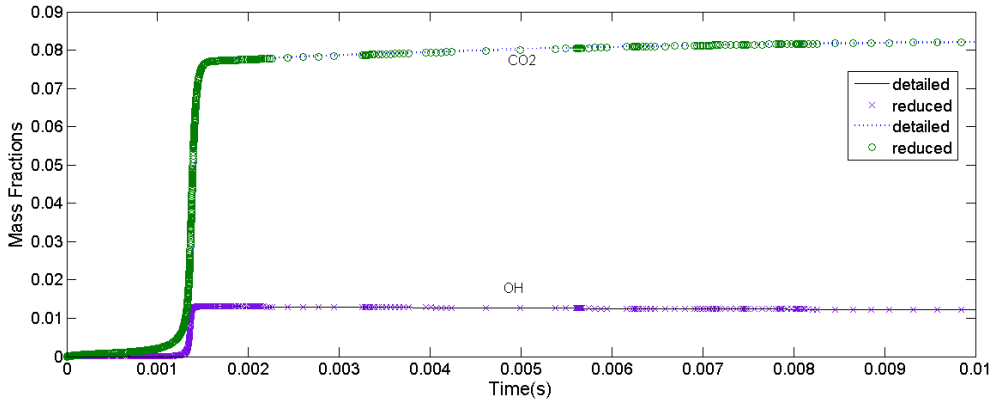

Figure 5.14. CO_2 and OH mass fractions at 0.1 atm for 1400 K starting temperature ignition.

Figure 5.13 and Figure 5.14 are the adiabatic, constant pressure ignition results for 1400 K starting temperature.The calculation of detailed mechanism takes 1283.8 s, skeletal mechanism cpu time is 25.6 s.

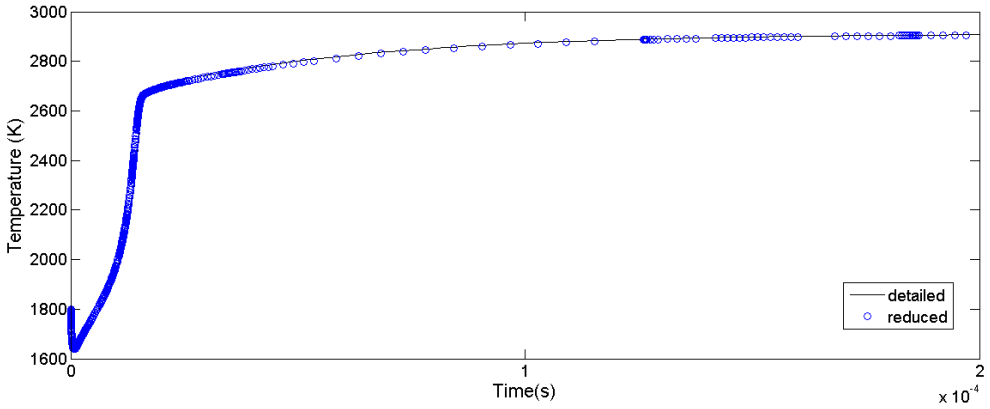

Figure 5.15. Adiabatic, constant pressure ignition result for 1800 K starting temperature at 1 atm.

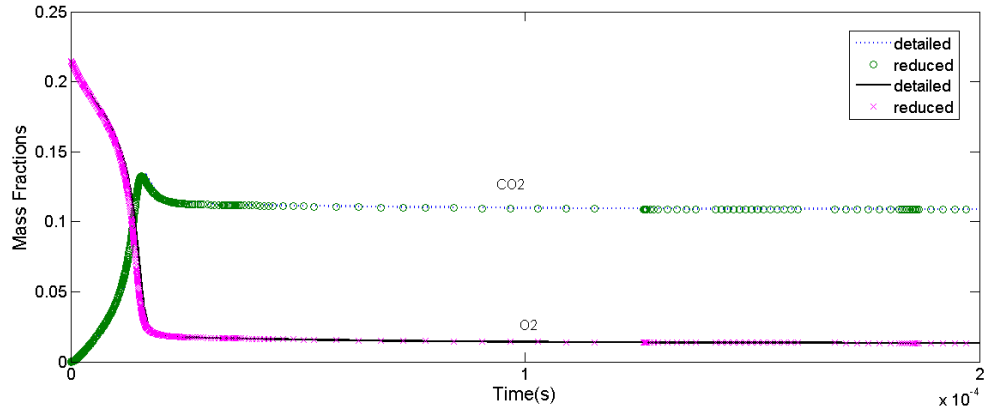

Figure 5.16. CO_2 and O_2 mass fractions at 1 atm for 1800 K starting temperature ignition.

Figure 5.15 and Figure 5.16 represent the adiabatic,constant pressure ignition results.Cpu time of detailed mechanism is 365.1 and cpu time of skeletal mechanism is 14.3 s.

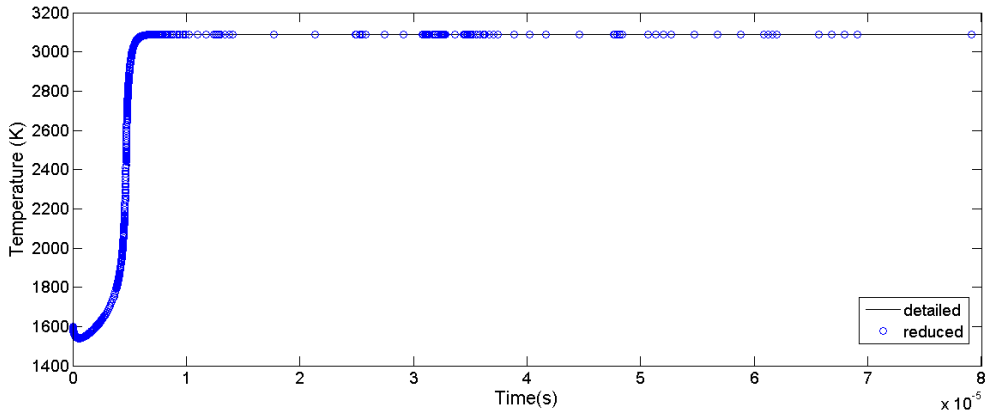

Figure 5.17. Adiabatic, constant pressure ignition result for 1600 K starting temperature at 30 atm.

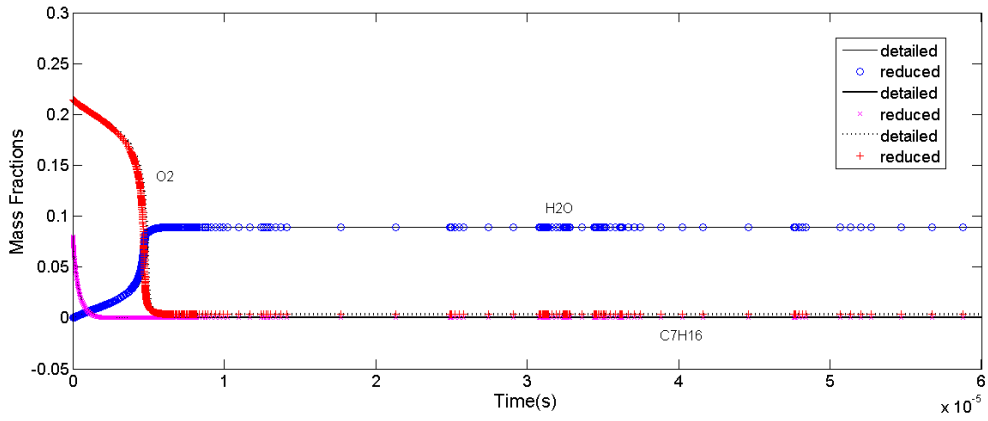

Figure 5.18. H_2O, C_7H_{16} and O_2 mass fractions at 30 atm for 1600 K starting temperature ignition.

Figure 5.17 and Figure 5.18 adiabatic,constant pressure ignition results for 1600 K starting temperature. Detailed mechanism cpu time is 294.2 and skeletal mechanism cpu time is 15.1 s. For $\Phi = 0.7$:

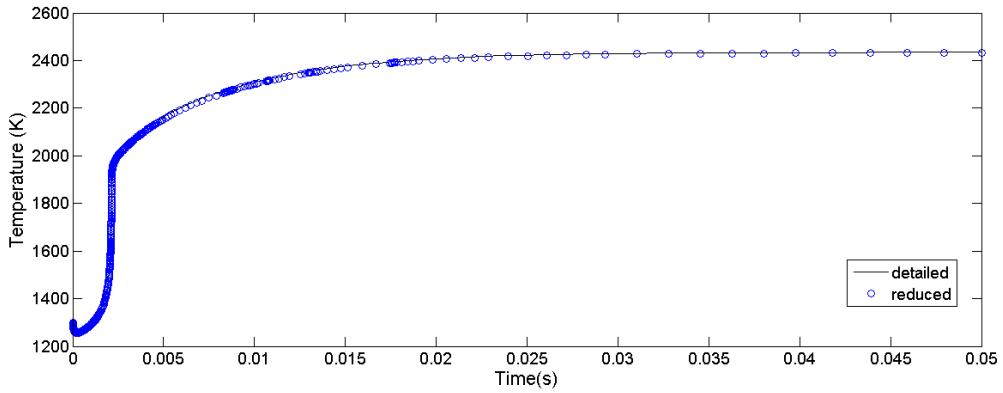

Figure 5.19. Adiabatic, constant pressure ignition result for 1300 K starting temperature at 0.1 atm.

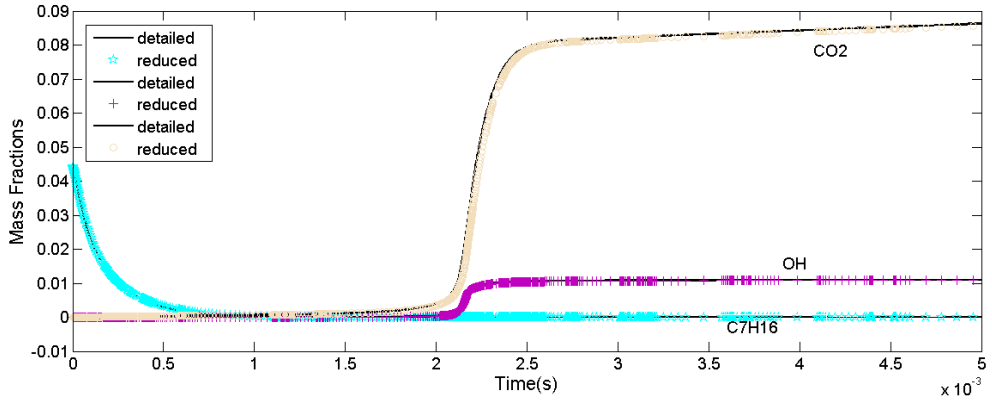

Figure 5.20. CO_2, C_7H_{16} and OH mass fractions at 0.1 atm for 1300 K starting temperature ignition.

Figure 5.19 and Figure 5.20 are the results of adiabatic ignition for constant pressure.Cpu time is 592.4 for detailed mechanism and is 19.2 for skeletal mechanism.

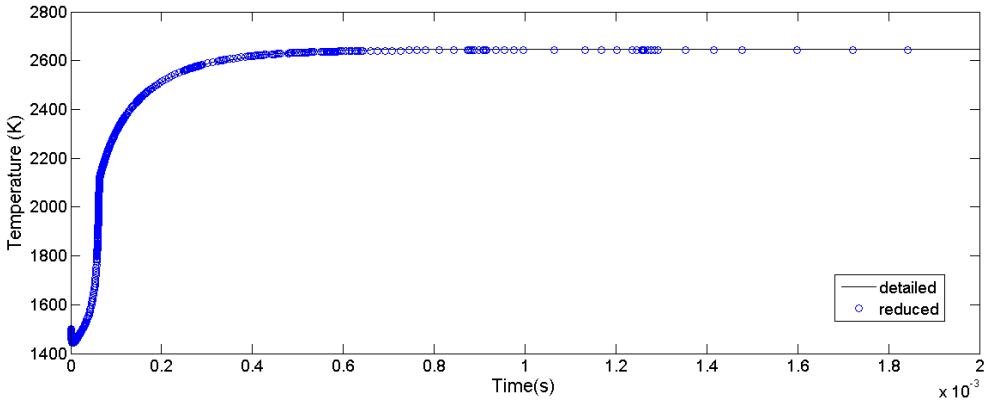

Figure 5.21. Adiabatic, constant pressure ignition result for 1500 K starting temperature at 1 atm.

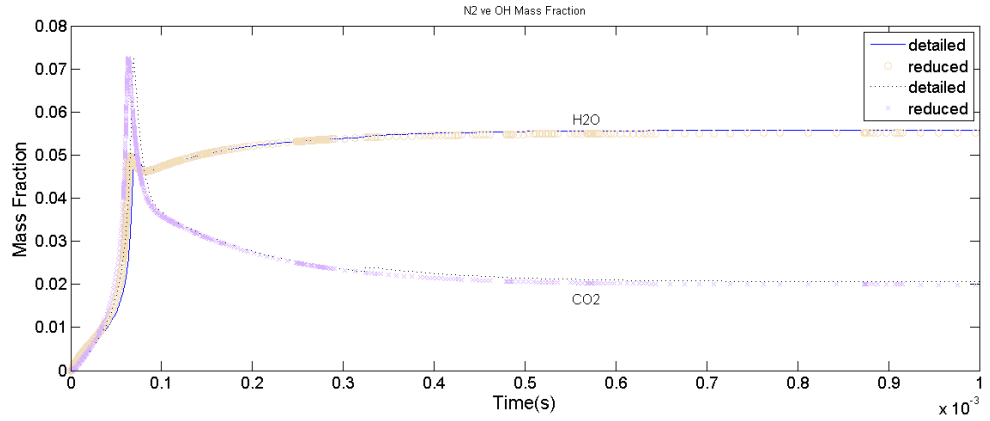

Figure 5.22. CO_2 and H_2O mass fractions at 1 atm for 1500 K starting temperature ignition.

Figure 5.21 and Figure 5.22 represent the calculation of adiabatic ignition results for constant pressure at 1500 K starting temperature.Detailed mechanism cpu time is 416.2 and skeletal mechanism cpu time is 25.8 s.

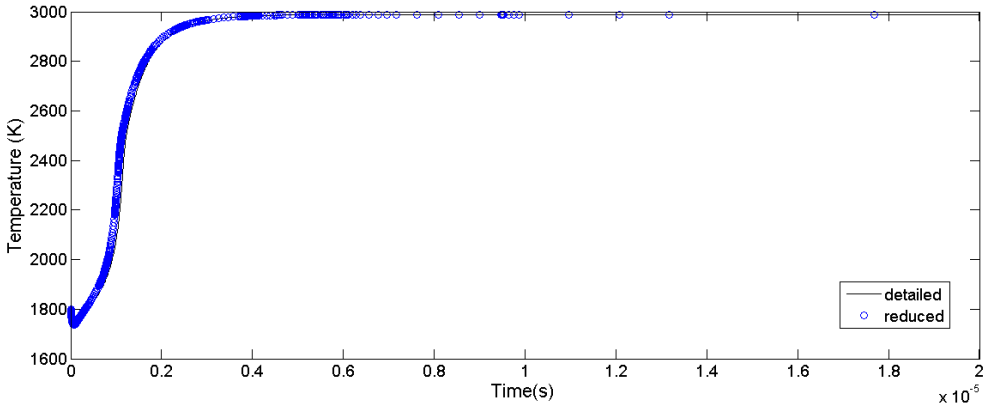

Figure 5.23. Adiabatic, constant pressure ignition result for 1800 K starting temperature at 30 atm.

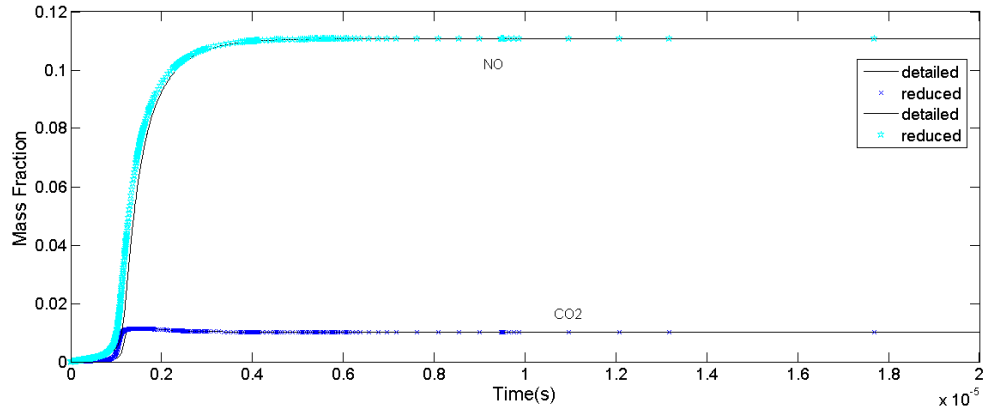

Figure 5.24. CO_2 and NO mass fractions at 30 atm for 1800 K starting temperature ignition.

Figure 5.23 and Figure 5.24 are the results of adiabatic, constant pressure ignition results st 1800 K starting temperature.Cpu time is 411.5 for detailed mechanism and cpu time is 14.4 for skeletal mechanism.

Results show that skeletal mechanism is well matched with the detailed mechanisms for variety of temperature, pressure and stoichiometric coefficients.

Table 5.2. CPU Times of the detailed and skeletal mechanism of n-heptane for different temperature, pressure and equilibrium cases at adiabatic constant pressure.

Temperature(K)	Pressure(Atm)	Equiviliance Ratio	Detailed Mechanism CPU Time(s)	Skeletal Mechanism CPU Time(s)
1700	0.1	1.0	1046.5	20.1
1400	1	1.0	522.4	14.2
1300	30	1.0	386.4	11.9
1400	0.1	1.3	1283.8	25.6
1800	1	1.3	365.1	14.4
1600	30	1.3	294.2	15.1
1300	0.1	0.7	592.4	19.2
1500	1	0.7	416.2	25.8
1800	30	0.7	411.5	14.4

Another important parameter is the ignition delay times. In the Figure 5.25, Figure 5.26 and Figure 5.27 are the ignition delay times of skeletal and detailed mechanism for different cases.

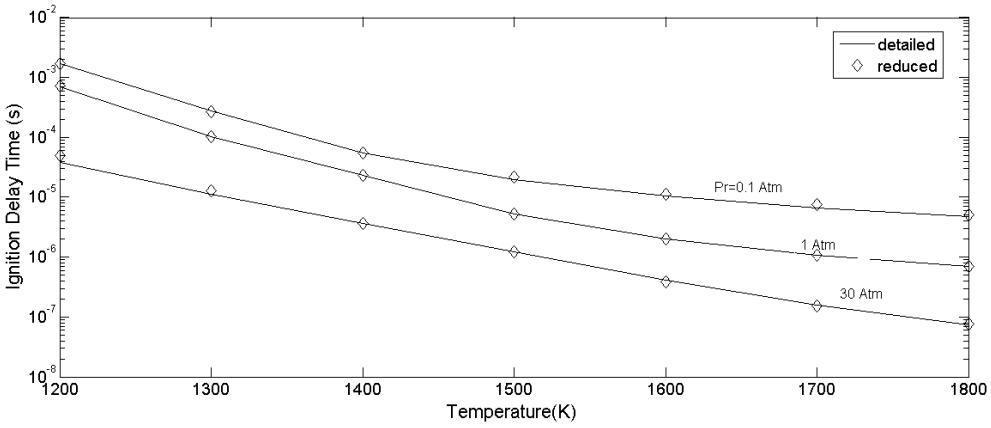

Figure 5.25. Ignition delay times for different pressure and temperature conditions for skeletal and detailed n-heptane mechanism at $\Phi = 0.7$.

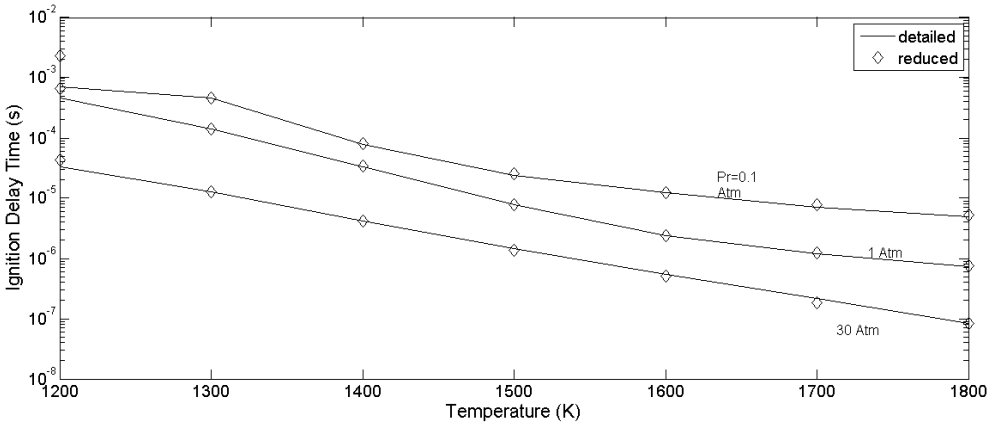

Figure 5.26. Ignition delay times for different pressure and temperature conditions for skeletal and detailed n-heptane mechanism at $\Phi = 1.0$.

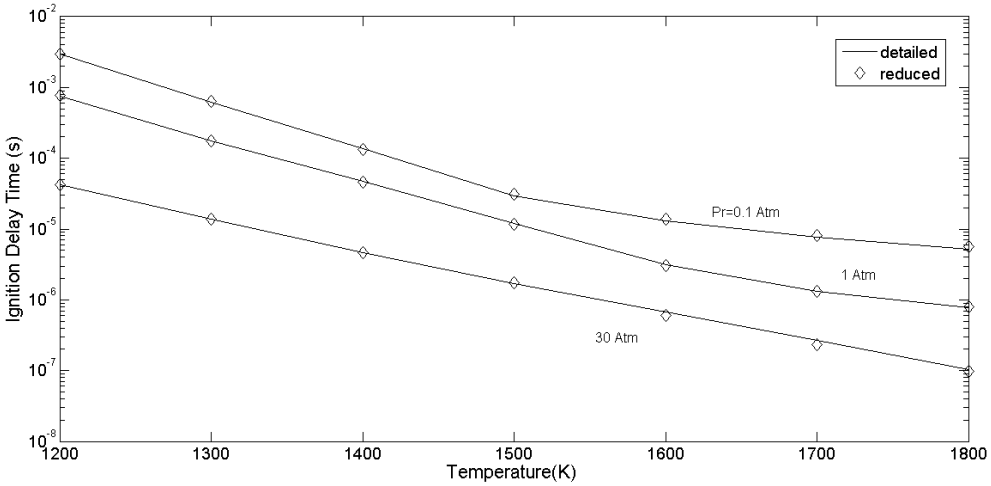

Figure 5.27. Ignition delay times for different pressure and temperature conditions for skeletal and detailed n-heptane mechanism at $\Phi = 1.3$.

6. CONCLUSION

Combustion simulations of higher molecular weight hydrocarbons is a challenging task due to large number of equations involved and due to the stiffness of the governing equations. It is desired to simplify the chemical kinetics to decrease the number of equations. In this thesis n-heptane was chosen as the target fuel of which the detailed chemical kinetics mechanism consists of 654 species and 4846 reversible reactions. This detailed mechanism is reduced using directed relation graph method (DRG). This method depends on species coupling and used extensively in the literature. Starting with a few initial species, (in our case NC7H16,AR,He and N2) a dependent set is found using DRG equations. This dependent set contains all the important species in order to calculate combustion of the n-heptane. Choosing the DRG parameter $\varepsilon = 0{:}13$, the dependent set contains 135 species. The skeletale chemical mechanism is formed with these 135 species by eliminating the reactions among the unused species. The resulting skeletal mechanism contains 1309 reversible reactions. This skeletal mechanism is validated for a large number of adiabatic constant pressure combustion cases. Results matched with detailed mechanism well and the errors in the calculations are less than % 1.

APPENDIX A: SKELETON MECHANISM

Species in the skeletal n-heptane mechanism for $\varepsilon = 0.13$

H H2 O O2 OH H2O N2 HO2 H2O2 AR
CO CO2 CH2O HCO
CH3O CH3O2H CH3O2 CH4 CH3 CH2
CH2(S) C2H6 C2H5 C2H4 C2H3 C2H2 C2H CH3CHO
CH3CO CH2CHO CH2CO HCCO C2H5O SC2H4OH C2H5O2
C2H3O1-2 CH3COCH3 CH3COCH2 C2H3CHO C2H3CO HE C3H8 IC3H7
NC3H7 C3H6 C3H5-A C3H5-S C3H5-T C3H4-P C3H4-A C3H3 C3H2
C3H5O C3H6OOH1-2 C3H6OOH1-2O2 NC3H7O2 IC3H7O2 C3H6O1-2
CH3CHCO C4H8-1 C4H8-2 PC4H9 SC4H9 C4H71-1 C4H71-2
C4H71-3 C4H71-4 C4H6 PC4H9O2 C4H7O PC4H8OH SC4H8OH NC3H7CO
C3H6CHO-2 SC3H5CHO SC3H5CO
TC3H6OH TC3H6O2HCO C5H11-1 C5H11-2 C5H10-1 C5H10-2
C5H81-3 C5H91-3 C5H91-4 C5H92-4 C5H9O1-3 C5H9O2-4 C5H11O2-1
C5H10OH-1 C5H10OH-2 O2C5H10OH-1 O2C5H10OH-2 C6H12-1
C6H12-2 C6H111-3 C6H112-4 C6H112-6 C6H113-1 NC4H9CHO NC4H9CO
C4H8CHO-2 C4H8CHO-3 C4H8CHO-4 NC7H16 C7H15-1 C7H15-2
C7H15-3 C7H15-4 C7H14-1 C7H14-2 C7H14-3 C7H131-3 C7H131-4
C7H132-4 C7H133-1 C7H133-5 C7H13O2-4 C7H13O3-5 C7H15O2-1
C7H15O2-2 C7H15O2-3 C7H15O2-4 C7H14OOH2-4 C7H14OOH2-4O2
C7H14O1-2 C7H14O1-3 C7H14O2-4 C5H91-1 C4H7CHO1-1 C4H7CO1-1
C4H6CHO1-14 C4H6CHO1-13 CHCHCHO C6H101-3

APPENDIX B: MATLAB CODE

Matlab code for directed relation graph

```
clc
clear all
T=[1100];
[a b]=size(T);
fi=[0.7 0.8 0.9 1.0 1.1 1.2 1.3];
[c d]=size(fi);
pt=[0.1 0.2 0.3 0.5 0.7 1.0 2.0 3.0 5.0 7.0 10 15 20 25 30]*oneatm;
[e f]=size(pt);
donguu=0
gas1=IdealGasMix('nc7_ver3.1_mech.xml');
i_nc7h16 = speciesIndex(gas1,'NC7H16');
i_o2 = speciesIndex(gas1,'O2');
i_ar = speciesIndex(gas1,'AR');
i_n2 = speciesIndex(gas1,'N2');
nsp = nSpecies(gas1);
Xi=zeros(1,nsp);
for hh=1:d
fiy=fi(hh);
a=(11/fiy);
Xi(i_nc7h16 )=1;
Xi(i_o2)=a;
Xi(i_n2)=3.76*a;
for k=1:f
pr=pt(k);
donguu=donguu+1
set(gas,'T',T,'P',pr,'X',Xi);
mw = molecularWeights(gas);
y0 = [temperature(gas) massFractions(gas)];
tel = [0 4];
options = odeset('RelTol',1.e-8,'AbsTol',1.e-15,'Stats','on');
t0 = cputime;
out = ode15s(@conhp,tel,y0,options,gas,mw);
```

```
33 disp(['CPU time = ' num2str(cputime - t0)]);
34 [b a]=size(Temperature1100{donguu});
35 Temper=zeros(1,a);
36 mole_fr=zeros(nsp,a);
37 Temper=Temperature1100{donguu}(1,:);
38 mole_fr=Temperature1100{donguu}(2 :end,:);
39 %%
40 %Finding 10 points
41 MaxT=max(Temper);
42 MinT=min(Temper);
43 MinT=single(MinT);
44 MaxT=single(MaxT);
45 Avg=(MaxT-MinT)/10;
46 D=MinT:Avg:MaxT;
47 rte=zeros(1,10);
48 index=zeros(1,10);
49 [rte(1),index(1)]=min(abs(Temper-D(1)));
50 [rte(2),index(2)]=min(abs(Temper-D(2)));
51 [rte(3),index(3)]=min(abs(Temper-D(3)));
52 [rte(4),index(4)]=min(abs(Temper-D(4)));
53 [rte(5),index(5)]=min(abs(Temper-D(5)));
54 [rte(6),index(6)]=min(abs(Temper-D(6)));
55 [rte(7),index(7)]=min(abs(Temper-D(7)));
56 [rte(8),index(8)]=min(abs(Temper-D(8)));
57 [rte(9),index(9)]=min(abs(Temper-D(9)));
58 [rte(10),index(10)]=min(abs(Temper-D(10)));
59 Tout(1)=Temper(index(1));
60 Tout(2)=Temper(index(2));
61 Tout(3)=Temper(index(3));
62 Tout(4)=Temper(index(4));
63 Tout(5)=Temper(index(5));
64 Tout(6)=Temper(index(6));
65 Tout(7)=Temper(index(7));
66 Tout(8)=Temper(index(8));
67 Tout(9)=Temper(index(9));
68 Tout(10)=Temper(index(10));
69 Tout(11)=Temper(a);
70 Tout(12)=Temper(1);
```

```
71 Xout(1,1:nsp)=mole_fr(:,(index(1)));
72 Xout(2,1:nsp)=mole_fr(:,(index(2)));
73 Xout(3,1:nsp)=mole_fr(:,(index(3)));
74 Xout(4,1:nsp)=mole_fr(:,index(4));
75 Xout(5,1:nsp)=mole_fr(:,index(5));
76 Xout(6,1:nsp)=mole_fr(:,index(6));
77 Xout(7,1:nsp)=mole_fr(:,index(7));
78 Xout(8,1:nsp)=mole_fr(:,index(8));
79 Xout(9,1:nsp)=mole_fr(:,index(9));
80 Xout(10,1:nsp)=mole_fr(:,index(10));
81 Xout(11,1:nsp)=mole_fr(:,a);
82 Xout(12,1:nsp)=mole_fr(:,1);
83 for zz=1:12
84 if (zz == 1 || zz==11)
85 zz
86 set(gas1,'T',Tout(zz),'P',pr,'Y',Xout(zz,:));
87 nu_r = stoich_r(gas1);
88 nu_p = stoich_p(gas1);
89 nu = stoich_net(gas1);
90 delta = nu_r + nu_p;
91 delta = delta ./ (delta+1E-30);
92 delta=full(delta);
93 omega = rop_net(gas1);
94 omega=transpose(omega);
95 for l=1:nsp
96 for n=1:nsp
97 total3=nu(l,:).*omega.*delta(n,:);
98 total3=abs(total3);
99 total3=sum(total3);
100 total1(l,n)=total3;
101 clear total3
102 end
103 end
104 omega=transpose(omega);
105 omega=abs(omega);
106 nu=abs(nu);
107 total2=nu*omega;
108 for dd=1:nsp
```

```
for vv=1:nsp
if (total2(dd)==0)
total4(dd,vv)=0;
else
total4(dd,vv)=total1(dd,vv)./total2(dd);
end
end
end
total4=full(total4);
if zz==1
k1Relative1100d4{donguu}=total4;
end
if zz==11
k11Relative1100d4{donguu}=total4;
end
clear gas1
clear total1
clear total2
clear total3
clear total4
save k1Relative1100d4{donguu}
save k11Relative1100d4{donguu}
gas1 = IdealGasMix('nc7_ver3.1_mech.xml');
end
end
end
end
```

```
load k1Total1100
load k11Total1100
i_nc7h16 = 396;
i_ar = 10;
i_n2 = 7;
epsilon=0.13;
dependent = i_nc7h16;
dependent_ar=i_ar;
dependent_n2=i_n2;
```

```
nsp = 654;
dongu=0
for i=1:105
r=k1Total1100{i};
re=sparse(nsp,nsp);
for n=1:nsp
for m=1:nsp
if r(m,n)> epsilon
if (r(m,n)==1.0)
if m==396 & n==396
r(m,n)=1.0;
end
r(m,n)=0.;
else
re(m,n)=r(m,n);
end
end
end
end
dongu=dongu+1;
dependent_nc7h16 = graphtraverse(re,i_nc7h16);
dependent = union(dependent, dependent_nc7h16);
dependent_ar = graphtraverse(re,i_ar);
dependent = union(dependent, dependent_ar);
dependent_n2 = graphtraverse(re,i_n2);
dependent = union(dependent, dependent_n2);
clear re
clear r
end
clear dependent_nc7h16
clear dependent_ar
clear dependent_n2
dependent_ar=i_ar;
dependent_n2=i_n2;
for k=1:105
r=k11Total1100{k};
re=sparse(nsp,nsp);
for n=1:nsp
```

```
for m=1:nsp
if r(m,n)> epsilon
if (r(m,n)==1.0)
if m==396 & n==396
r(m,n)=1.0;
end
r(m,n)=0.;
else
re(m,n)=r(m,n);
end
end
end
end
dongu=dongu+1;
dependent_nc7h16 = graphtraverse(re,i_nc7h16);
dependent = union(dependent, dependent_nc7h16);
dependent_ar = graphtraverse(re,i_ar);
dependent = union(dependent, dependent_ar);
dependent_n2 = graphtraverse(re,i_n2);
dependent = union(dependent, dependent_n2);
clear re
clear r
end
clearvars -except dependent
dependent1100=dependent
clear dependent
save dependent051100
clear all
clc
```

REFERENCES

1. Smoot, L. D., "Role of combustion research in the fossil energy industry", *Energy & fuels*, Vol. 7, No. 6, pp. 689–699, 1993.

2. Turns, S., *An introduction to combustion: concepts and applications*, McGraw-Hill series in mechanical engineering, McGraw-Hill ,New Delhi, 1996.

3. Strehlow, R., *Combustion fundamentals*, McGraw-Hill series in energy, combustion, and environment, McGraw-Hill, New York, NY, 1984.

4. Glassman, I., *Combustion*, Energy series, Academic Press, London, UK, 1977.

5. Law, C., *Combustion Physics*, Cambridge University Press, Cambridge, UK, 2006.

6. Hiremath, V., Z. Ren and S. B. Pope, "A greedy algorithm for species selection in dimension reduction of combustion chemistry", *Combustion Theory and Modelling*, Vol. 14, No. 5, pp. 619–652, 2010.

7. Karadeniz, H., H. S. Soyhan and C. Sorusbay, "Reduction of large kinetic mechanisms with a new approach to the necessity analysis method", *Combustion and Flame*, Vol. 159, No. 4, pp. 1467–1480, 2012.

8. Hiremath, V. and S. B. Pope, "A study of the rate-controlled constrained-equilibrium dimension reduction method and its different implementations", *Combustion Theory and Modelling*, Vol. 17, No. 2, pp. 260–293, 2013.

9. Turányi, T., "Sensitivity analysis of complex kinetic systems. Tools and applications", *Journal of Mathematical Chemistry*, Vol. 5, No. 3, pp. 203–248, 1990.

10. Okino, M. S. and M. L. Mavrovouniotis, "Simplification of mathematical models of chemical reaction systems", *Chemical reviews*, Vol. 98, No. 2, pp. 391–408, 1998.

11. Seiser, R., H. Pitsch, K. Seshadri, W. Pitz and H. Gurran, "Extinction and autoignition of n-heptane in counterflow configuration", *Proceedings of the Combustion Institute*, Vol. 28, No. 2, pp. 2029–2037, 2000.

12. Maroteaux, F. and L. Noel, "Development of a reduced n-heptane oxidation mechanism for HCCI combustion modeling", *Combustion and Flame*, Vol. 146, No. 1, pp. 246–267, 2006.

13. Zheng, X., T. Lu and C. Law, "Experimental counterflow ignition temperatures and reaction mechanisms of 1, 3-butadiene", *Proceedings of the Combustion Institute*, Vol. 31, No. 1, pp. 367–375, 2007.

14. Lu, T. and C. K. Law, "Toward accommodating realistic fuel chemistry in large-scale computations", *Progress in Energy and Combustion Science*, Vol. 35, No. 2, pp. 192–215, 2009.

15. Turanyi, T., "Reduction of large reaction mechanisms", *New journal of chemistry*, Vol. 14, No. 11, pp. 795–803, 1990.

16. Dibble, R., J. Warnatz and U. Maas, *Combustion: physical and chemical fundamentals, modelling and simulations, experiments, pollutant formation*, Springer, New York, NY, 1996.

17. Zeuch, T., G. Moréac, S. S. Ahmed and F. Mauss, "A comprehensive skeletal mechanism for the oxidation of n-heptane generated by chemistry-guided reduction", *Combustion and Flame*, Vol. 155, No. 4, pp. 651–674, 2008.

18. Xi, J. and B.-J. Zhong, "Reduced kinetic mechanism of n-heptane oxidation in modeling polycyclic aromatic hydrocarbon formation in diesel combustion", *Chemical engineering & technology*, Vol. 29, No. 12, pp. 1461–1468, 2006.

19. Sun, W., Z. Chen, X. Gou and Y. Ju, "A path flux analysis method for the reduction of detailed chemical kinetic mechanisms", *Combustion and Flame*, Vol. 157,

No. 7, pp. 1298–1307, 2010.

20. Luche, J., M. Reuillon, J.-C. Boettner and M. Cathonnet, "Reduction of large detailed kinetic mechanisms: application to kerosene/air combustion", *Combustion science and technology*, Vol. 176, No. 11, pp. 1935–1963, 2004.

21. Niemeyer, K. E. and C.-J. Sung, "On the importance of graph search algorithms for DRGEP-based mechanism reduction methods", *Combustion and Flame*, Vol. 158, No. 8, pp. 1439–1443, 2011.

22. Pepiot, P. and H. Pitsch, "Systematic reduction of large chemical mechanisms", *4th joint meeting of the US Sections of the Combustion Institute, Philadelphia, PA*, 2005.

23. Niemeyer, K. E., C.-J. Sung and M. P. Raju, "Skeletal mechanism generation for surrogate fuels using directed relation graph with error propagation and sensitivity analysis", *Combustion and flame*, Vol. 157, No. 9, pp. 1760–1770, 2010.

24. Lu, T., M. Plomer, Z. Luo, S. Sarathy, W. Pitz, S. Som and D. E. Longman, "Directed relation graph with expert knowledge for skeletal mechanism reduction", *7th US National Combustion Meeting*, 2011.

25. Lu, T. and C. K. Law, "Linear time reduction of large kinetic mechanisms with directed relation graph: n-Heptane and iso-octane", *Combustion and Flame*, Vol. 144, No. 1, pp. 24–36, 2006.

26. Lu, T. and C. K. Law, "On the applicability of directed relation graphs to the reduction of reaction mechanisms", *Combustion and Flame*, Vol. 146, No. 3, pp. 472–483, 2006.

27. Lu, T. and C. K. Law, "Strategies for mechanism reduction for large hydrocarbons: n-heptane", *Combustion and flame*, Vol. 154, No. 1, pp. 153–163, 2008.

28. Xin, Y., Z. Song, Y. Tan and D. Wang, "The directed relation graph method for mechanism reduction in the oxidative coupling of methane", *Catalysis Today*, Vol. 131, No. 1, pp. 483–488, 2008.

29. Lu, T. and C. K. Law, "A directed relation graph method for mechanism reduction", *Proceedings of the Combustion Institute*, Vol. 30, No. 1, pp. 1333–1341, 2005.

30. Luo, Z., M. Plomer, T. Lu, S. Som, D. E. Longman, S. M. Sarathy and W. J. Pitz, "A reduced mechanism for biodiesel surrogates for compression ignition engine applications", *Fuel*, Vol. 99, pp. 143–153, 2012.

31. Abdelouahad Ait, M., B. Abdeltif, M. Mustapha, A. Elhoussin and M. M'hamed, "Reduced detailed mechanism for methane combustion", *Energy and Power Engineering*, Vol. 2012, 2012.

32. Pepiot-Desjardins, P. and H. Pitsch, "An efficient error-propagation-based reduction method for large chemical kinetic mechanisms", *Combustion and Flame*, Vol. 154, No. 1, pp. 67–81, 2008.

33. Niemeyer, K. E. and C.-J. Sung, "Mechanism reduction for multicomponent surrogates: A case study using toluene reference fuels", *Combustion and Flame*, Vol. 161, No. 11, pp. 2752–2764, 2014.

34. Liu, W., R. Sivaramakrishnan, M. J. Davis, S. Som, D. Longman and T. Lu, "Development of a reduced biodiesel surrogate model for compression ignition engine modeling", *Proceedings of the Combustion Institute*, Vol. 34, No. 1, pp. 401–409, 2013.

35. Houshfar, E., Ø. Skreiberg, P. Glarborg and T. Løvås, "Reduced chemical kinetic mechanisms for NOx emission prediction in biomass combustion", *International Journal of Chemical Kinetics*, Vol. 44, No. 4, pp. 219–231, 2012.

36. Valorani, M., H. N. Najm and D. A. Goussis, "CSP analysis of a transient flame-vortex interaction: time scales and manifolds", *Combustion and Flame*, Vol. 134, No. 1, pp. 35–53, 2003.

37. Lam, S. and D. Goussis, "The CSP method for simplifying kinetics", *International Journal of Chemical Kinetics*, Vol. 26, No. 4, pp. 461–486, 1994.

38. Lam, S. H., "Model reductions with special CSP data", *Combustion and Flame*, Vol. 160, No. 12, pp. 2707–2711, 2013.

39. "LLNL Detailed Mechanism of N-Heptane", 2011, `https://combustion.llnl.gov/mechanisms/alkanes/n-heptane-detailed-mechanism-version-3`, [Accessed August 2015].